

# UC Berkeley

## UC Berkeley Previously Published Works

### Title

Metastable Ta<sub>2</sub>N<sub>3</sub> with highly tunable electrical conductivity via oxygen incorporation

### Permalink

<https://escholarship.org/uc/item/3vc240q3>

### Journal

Materials Horizons, 8(6)

### ISSN

2051-6347

### Authors

Jiang, Chang-Ming  
Wagner, Laura I  
Horton, Matthew K  
[et al.](#)

### Publication Date

2021-06-01

### DOI

10.1039/d1mh00017a

Peer reviewed


## Ion Correlations and Their Impact on Transport in Polymer-Based Electrolytes

Kara D. Fong, Julian Self, Bryan D. McCloskey, and Kristin A. Persson\*


 Cite This: <https://dx.doi.org/10.1021/acs.macromol.0c02545>

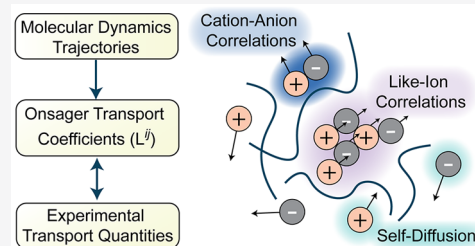
 Read Online

ACCESS |


 Metrics & More


 Article Recommendations

**ABSTRACT:** The development of next-generation polymer-based electrolytes for energy storage applications would greatly benefit from a deeper understanding of transport phenomena in these systems. In this Perspective, we argue that the Onsager transport equations provide an intuitive but underutilized framework for analyzing transport in polymer-based electrolytes. Unlike the ubiquitous Stefan–Maxwell equations, the Onsager framework generates transport coefficients with clear physical interpretation at the atomistic level and can be computed easily from molecular simulations using Green–Kubo relations. Herein we present an overview of the Onsager transport theory as it applies to polymer-based electrolytes and discuss its relation to experimentally measurable transport properties and the Stefan–Maxwell equations. Using case studies from recent computational work, we demonstrate how this framework can clarify nonintuitive phenomena such as negative cation transference number, anticorrelated cation–anion motion, and the dramatic failure of the Nernst–Einstein approximation. We discuss how insights from such analysis can inform design rules for improved systems.



### INTRODUCTION

Polymer-based electrolytes play a crucial role in a wide range of systems, including energy storage devices,<sup>1–5</sup> membrane-based separation technology,<sup>6–9</sup> and biological processes and applications.<sup>10–13</sup> These materials include solid polymer electrolytes, which consist of salts dissolved in a high molecular weight polymer host, as well as polyionic systems, where one of the ions is incorporated into a polymer chain. The latter, typically called single-ion conductors, may be dry or include additional solvent to form either a gel or a fully dissolved polyelectrolyte solution.<sup>1,14</sup> For the specific case of energy storage applications such as batteries, the adoption of polymer-based electrolytes is largely limited by the transport properties of these systems.<sup>1,15</sup> Poor transport can result in additional overpotentials and detrimental concentration gradients that can limit the efficiency and rate capability of the device.<sup>16,17</sup>

The development of enhanced polymer-based electrolytes is contingent on a multifaceted understanding of the transport phenomena in these systems: we require both a continuum-level description of transport to predict macroscopic concentration and potential profiles and a molecular-level description to gain insight into the mechanisms governing transport. However, there often exists a disconnect between the techniques used at these two levels. Experimental results and finite-element models most commonly describe transport using the Stefan–Maxwell equations.<sup>17–19</sup> While these equations are adequate for continuum-level modeling, interpretation of the Stefan–Maxwell transport coefficients at the atomistic level is challenging.<sup>20,21</sup> Molecular simulations probe transport at the

level of ion positions and velocities and thus offer detailed resolution into transport mechanisms, but it is not straightforward to generate Stefan–Maxwell coefficients from simulation trajectories.<sup>22,23</sup>

We argue that the Onsager transport equations provide a powerful framework for rigorously analyzing transport in electrolytes at both the continuum and molecular levels.<sup>23–28</sup> These transport equations are written in terms of Onsager transport coefficients,  $L^{ij}$ , which quantify correlations in ion motion and are directly accessible from molecular simulations. While this framework has thus far proven useful in a handful of electrolyte studies,<sup>29–34</sup> its use is by no means common, particularly for polymer-based electrolytes. Given this opportunity to more effectively analyze transport in polymer electrolytes, the primary objectives of this Perspective are as follows: (i) We provide an overview of the Onsager transport equations, establishing how the Onsager transport coefficients  $L^{ij}$  relate to molecular dynamics (MD) trajectories, experimentally measurable transport quantities, and the Stefan–Maxwell transport coefficients. (ii) We demonstrate the types of insights that can be obtained from analyzing ion transport

Received: November 16, 2020

Revised: January 30, 2021

through the lens of Onsager transport coefficients in polymer-based electrolytes. We emphasize cases in which ion correlations and the transport coefficients quantifying them can rationalize particularly counterintuitive transport phenomena, such as negative transference numbers, anticorrelated cation–anion motion, and the drastic failure of commonly used dilute solution approximations. In addition, we provide guidance on how these insights may be used to inform the design of improved systems. As ion correlations and transport coefficients can be probed most directly through molecular simulations, this Perspective focuses largely on studies employing atomistic and coarse-grained molecular dynamics, including our group's previous work simulating polyelectrolyte solutions as well as other investigators' recent computational studies on transport in polymerized ionic liquids, ionomer melts, and solid polymer electrolytes. This text is not intended to provide a comprehensive review of the literature, and we refer the reader to several of the review articles on transport phenomena in polymer-based and small-molecule electrolytes published in recent years.<sup>14,15,32,35–38</sup> Rather, our aim is that this Perspective will encourage more widespread adoption of transport coefficient analysis to ultimately enable the development of next-generation polymer-based electrolytes.

## THEORY OF ION TRANSPORT

Transport phenomena, whether it be for transport of mass, momentum, or heat, are most generally understood in terms of linear laws relating forces and fluxes within a system.<sup>24–26,39</sup> One of the most familiar linear laws of transport behavior is Fick's law of diffusion. Here, the thermodynamic driving force acting on species  $i$  is the gradient in concentration  $c_i$ , which is linearly related to the flux of species  $i$ ,  $J_i$ , via the diffusion coefficient  $D_i$ :

$$J_i = -D_i \nabla c_i \quad (1)$$

The flux may be written in terms of the average velocity of species  $i$ ,  $v_i$ , as  $J_i = c_i(v_i - v)$ , where  $v$  is the mass-averaged (center-of-mass) velocity of the system. Equation 1 is only applicable to an ideal solution of uncharged particles.

To describe transport in electrolyte solutions, we must formulate linear laws analogous to eq 1 which account for solution nonideality (activity coefficients not equal to one), including electrostatic interactions and short-ranged chemical interactions between species. The Onsager transport equations<sup>23–28</sup> capture these effects and provide a means of fully characterizing electrolyte transport:

$$J_i = -\sum_j L^{ij} \nabla \bar{\mu}_j \quad (2)$$

We note several key differences between eq 2 and Fick's law (eq 1). First, the thermodynamic driving force has been transformed from the gradient in concentration to the gradient in electrochemical potential,  $\bar{\mu}_j$ . The electrochemical potential incorporates effects from the chemical potential  $\mu_j$ , which accounts for nonidealities, and the electric potential  $\phi$ , such that  $\bar{\mu}_j = \mu_j + z_j F \phi$ , where  $z_j$  is the charge valence of species  $j$  and  $F$  is Faraday's constant. We note that the electric potential  $\phi$  as defined herein is the result of an externally applied electric field  $E = -\nabla \phi$  and that the effects of microscopic potential gradients due to individual ion interactions and local dielectric heterogeneities are captured in the chemical potential  $\mu_j$ .<sup>40</sup> Second, whereas the right-hand side of Fick's law (eq 1) includes only one term, the right side of the Onsager transport equations

(eq 2) features a sum over all species  $j$  in the system. This sum captures interactions between different species, accounting for the fact that a gradient in electrochemical potential of species  $j$  may induce a flux of species  $i \neq j$ . In electrolytes, where the electrostatic attraction between ions induces inherent correlations between different species' motion, these cross-terms are significant. Because the Onsager transport equations capture cross-correlations, the transport coefficients can no longer be scalars such as  $D_i$ . Rather, we obtain a matrix of transport coefficients, with one coefficient for each pair of species. These Onsager transport coefficients are called  $L^{ij}$ . This theory will be applicable in the bulk of a well-mixed electrolyte; we refer the reader to the text by Kjelstrup and Bedeaux<sup>41</sup> for a discussion of nonequilibrium thermodynamics in heterogeneous systems.

Note that in some works<sup>31,32,42</sup> the Onsager transport coefficients are denoted by  $\sigma^{ij}$ , related to  $L^{ij}$  via  $L^{ij} = \frac{\sigma^{ij}}{z_i z_j F^2}$ , such that the transport coefficients exhibit the dimensions of ionic conductivity. Furthermore, it is also common to express the transport equations in terms of concentration gradients, rather than electrochemical potential gradients, to yield a transport equation more similar to Fick's law:<sup>43</sup>  $J_i = -\rho \sum_j \mathbb{D}^{ij} \nabla c_j$ , where  $\mathbb{D}^{ij}$  are the mutual diffusion coefficients and  $\rho$  is the mass density. The mutual diffusion coefficients and Onsager transport coefficients may be related by

$$\mathbb{D}^{ij} = \frac{1}{\rho} \sum_k \left( \frac{\partial \bar{\mu}_i}{\partial c_k} \right) L^{ik}.$$

In the remainder of this section, we discuss the relationship between the Onsager transport coefficients and (i) molecular simulations, (ii) experimental transport quantities, and (iii) alternate transport frameworks, namely the Stefan–Maxwell equations. These relationships are outlined in Figure 1.

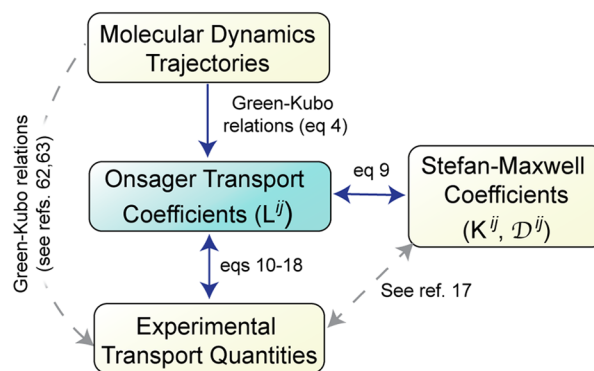


**Figure 1.** Outline of the relationships between the Onsager transport coefficients and other aspects of transport.

**Computing Transport Coefficients from Molecular Simulations.** In general, transport coefficients are accessible from molecular simulations through Green–Kubo relations, which enable calculation of nonequilibrium transport properties from fluctuations at equilibrium. One familiar example is the relation for the self-diffusion coefficient:

$$\begin{aligned} D_i &= \frac{1}{3} \int_0^\infty dt \langle (v_i(t) - v(t)) \cdot (v_i(0) - v(0)) \rangle \\ &= \frac{1}{6N_i} \lim_{t \rightarrow \infty} \frac{d}{dt} \left\langle \sum_\alpha [r_i^\alpha(t) - r_i^\alpha(0)]^2 \right\rangle \end{aligned} \quad (3)$$

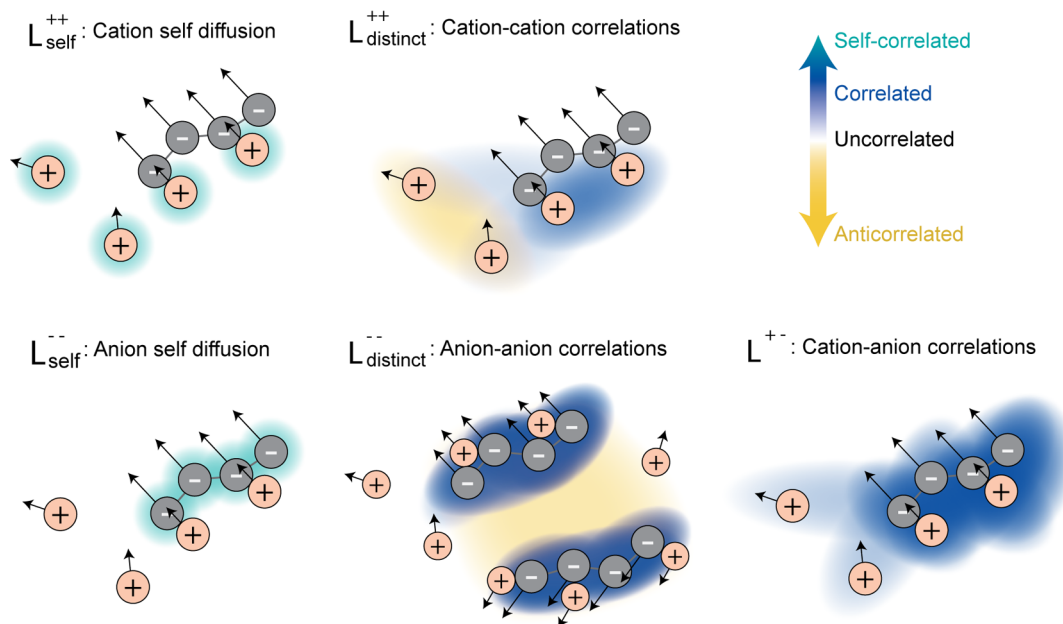


**Figure 2.** Schematic illustration of the types of ion motion and correlations captured by each transport coefficient  $L^j$ . The color bar in the upper right qualitatively indicates the type of ion correlation (or lack thereof), and the arrows on each ion indicate direction of motion. Reproduced with permission from ref 30.

The first form of the equation gives the diffusion coefficient as the integral of the velocity autocorrelation function of species  $i$  over time (we recall that  $v_i$  is the average velocity of all atoms/molecules of type  $i$ ). The second form, called the Einstein relation, is more commonly used in molecular simulations and is written in terms of  $N_i$ , the number of atoms/molecules of type  $i$  in the system, and  $r_i^\alpha$ , defined as the position (relative to the system center-of-mass) of particle  $\alpha$  of type  $i$ . The term in angular brackets is the mean-squared displacement, the slope of which is proportional to the diffusion coefficient. Experimentally, the self-diffusion coefficient is typically measured by using pulsed-field gradient nuclear magnetic resonance (NMR).<sup>44–47</sup>

There exist analogous Green–Kubo relations for computing the Onsager transport coefficients as well:<sup>22,23,43,48,49</sup>

$$L^j = \frac{V}{3k_B T} \int_0^\infty dt \langle J_i(t) \cdot J_j(0) \rangle \quad (4)$$

where  $k_B T$  is the thermal energy and  $V$  is volume. The derivation of this relation can be found in Fong et al.<sup>23</sup> Here, too, we can rewrite this equation in the form of an Einstein relation in terms of individual particle positions rather than velocities:

$$L^j = \frac{1}{6k_B T V} \lim_{t \rightarrow \infty} \frac{d}{dt} \left\langle \sum_\alpha [r_i^\alpha(t) - r_i^\alpha(0)] \cdot \sum_\beta [r_j^\beta(t) - r_j^\beta(0)] \right\rangle \quad (5)$$

As is clear from these relations,  $L^{ij} = L^{ji}$ ; this is an example as the Onsager reciprocal relations.<sup>24,25</sup> Furthermore, note that all of the equations thus far utilize a barycentric reference frame; that is, all velocities (positions) are relative to the center-of-mass velocity (position) of the entire system. As a consequence of this reference frame, where all mass fluxes sum to zero, the transport coefficients are subject to the constraint that  $\sum_i M_i L^j = 0$ , where  $M_i$  is the molar mass of species  $i$ . Thus, an  $n$ -component isotropic system will have only  $n(n-1)/2$  independent transport coefficients. A binary salt and solvent electrolyte, for example, will have three independent transport coefficients:  $L^{+-}$ ,  $L^{++}$ , and  $L^{--}$ .

Rigorous calculation of  $L^j$  requires a simulation long enough to reach the diffusive regime; that is, the term in angular brackets in eq 5 must be linear with respect to time. This requirement can be challenging to meet in many polymer-based systems with slow dynamics. Furthermore, unlike the self-diffusion coefficient, calculation of  $L^j$  does not entail averages over all particles of a given type and is thus subject to increased statistical noise. The diffusive regime has been shown to be accessible for systems with short chains and reasonably fast dynamics, although it is typically necessary to perform many replicate simulations to achieve reasonable error estimates.<sup>29,30,50</sup> Even when the diffusive regime is not accessible, however, we can still obtain valuable insight from  $L^j$  by generating approximate values and comparing the relative magnitudes of each transport coefficient across different systems;<sup>33</sup> for example, one can simply compare the magnitude of the term in the angular brackets in eq 5. The analogous practice of comparing the mean-squared displacement as a proxy for rigorously computing the self-diffusion coefficient in systems that do not reach the diffusive regime is common in the literature for solid polymer electrolytes.<sup>51–54</sup>

**Physical Interpretation of  $L^j$ .** The Onsager transport coefficients  $L^j$  capture correlations in the motion of species  $i$  and  $j$ . This physical interpretation is illustrated schematically in Figure 2. In what follows, we describe each of these transport coefficients individually. Although the schematics in Figure 2 are for the specific case of a polyanionic system, the discussion below is readily generalized to any other polymer-based electrolyte.

We first discuss the transport coefficients where  $i = j$ ,  $L^{ii}$ . At the level of individual ions' motion, contributions to  $L^{ii}$  arise from two sources, deemed self and distinct:  $L^{ii} = L_{\text{self}}^{ii} + L_{\text{distinct}}^{ii}$ . Mathematically, these two contributions arise from splitting the double summation in eq 5 into the cases where  $\alpha = \beta$  (the self term) and  $\alpha \neq \beta$  (the distinct term). The self term may be interpreted as capturing ideal, uncorrelated particle motion and is directly related to the self-diffusion coefficient of the species (Table 1). The distinct term corresponds to correlations

**Table 1.** Experimentally Measurable Transport Quantities and How Each May Be Obtained from Onsager Transport Coefficients  $L^{ij}$  in a Binary Electrolyte

transport quantity	expression <sup>a</sup> in terms of $L^{ij}$	ideal solution expression <sup>b</sup>
self-diffusion coefficient ( $D_i$ )	$D_i = \frac{RT}{c_i} L_{\text{self}}^{ii}$ (10)	$D_i^{\text{NE}} = D_i = \frac{RT}{c_i} L_{\text{self}}^{ii}$ (11)
ionic conductivity ( $\sigma$ )	$\sigma = F^2(z_+^2 L^{++} + z_-^2 L^{--} + 2z_+ z_- L^{+-})$ (12)	$\sigma^{\text{NE}} = F^2(z_+^2 L_{\text{self}}^{++} + z_-^2 L_{\text{self}}^{--}) = \frac{F^2 c}{RT} (z_+^2 D_+ + z_-^2 D_-)$ (13)
cation transference number ( $t_+$ )	$t_+ = \frac{z_+^2 L^{++} + z_+ z_- L^{+-}}{z_+^2 L^{++} + z_-^2 L^{--} + 2z_+ z_- L^{+-}}$ (14)	$t_+^{\text{NE}} = \frac{z_+^2 L_{\text{self}}^{++}}{z_+^2 L_{\text{self}}^{++} + z_-^2 L_{\text{self}}^{--}} = \frac{z_+ D_+}{z_+ D_+ + z_- D_-}$ (15)
salt diffusion coefficient ( $D_{\text{salt}}$ )	$D_{\text{salt}} = \frac{\nu RT}{c \nu_+ \nu_-} \xi \left( \frac{-z_+ z_- (L^{++} L^{--} - L^{+-2})}{z_+^2 L^{++} + z_-^2 L^{--} + 2z_+ z_- L^{+-}} \right)$ (16)	$D_{\text{salt}}^{\text{NE}} = \left( \frac{\nu RT}{c} \right) \frac{-z_+ z_- L_{\text{self}}^{++} L_{\text{self}}^{--}}{\nu_+ \nu_- (z_+^2 L_{\text{self}}^{++} + z_-^2 L_{\text{self}}^{--})} = \left( \frac{\nu}{\nu_+ \nu_-} \right) \frac{-z_+ z_- D_+ D_-}{z_+^2 D_+ + z_-^2 D_-}$ (17)
ionicity ( $\sigma/\sigma^{\text{NE}}$ )	$\sigma/\sigma^{\text{NE}} = \frac{(z_+^2 L^{++} + z_-^2 L^{--} + 2z_+ z_- L^{+-})}{c/RT(z_+^2 D_+ + z_-^2 D_-)}$ (18)	$\sigma/\sigma^{\text{NE}} = 1$ (19)

<sup>a</sup>List of symbols: Faraday's constant ( $F$ ), charge valence of species  $i$  ( $z_i$ ), salt concentration ( $c = c_+/\nu_+ = c_-/\nu_-$ ), thermal energy ( $RT$ ), thermodynamic factor ( $\xi = 1 + \frac{d \ln f_{\text{salt}}}{d \ln c}$ ), salt activity coefficient ( $f_{\text{salt}}$ ), stoichiometric coefficients of ion  $i$  in salt ( $\nu_i$ ,  $\nu = \nu_+ + \nu_-$ ). <sup>b</sup>In an ideal solution, we apply the Nernst–Einstein approximation, which states that there are no correlations between species ( $L_{\text{distinct}}^{ij}$  and  $L^{ij}$ ,  $i \neq j$  are zero). We further assume a salt activity coefficient of one.

between different particles of the same species. Consider  $L_{\text{distinct}}^{++}$  in the case of a polyanionic electrolyte as shown in Figure 2 (upper middle panel). In general, two distinct cations will move in an anticorrelated manner due to electrostatic repulsion, as illustrated by the yellow shading between the two free cations in the figure. This will yield a negative contribution to  $L_{\text{distinct}}^{++}$ . The motion of two cations which are part of the same aggregate (in this case ionically bound to the same polyanion chain), however, will be positively correlated ( $L_{\text{distinct}}^{++} > 0$ , indicated by blue shading in the figure). The intuition governing  $L_{\text{distinct}}^{--}$  (Figure 2, lower middle panel) is similar. Distinct polyanionic chains will electrostatically repel and thus be anticorrelated, whereas anions within a given chain will be very strongly correlated.

The transport coefficients in which  $i \neq j$  quantify correlations between different types of species. Herein we consider only  $L^{+-}$ , describing cation–anion correlation in a binary salt solution. With the exception of certain systems which will be discussed below,  $L^{+-}$  is generally positive due to the electrostatic attraction between cations and anions (Figure 2, lower right panel). This correlation will be strongest for ions that are directly paired, although long-range electrostatic interactions will also contribute to  $L^{+-}$ . Note that  $L^{+-}$  captures the total extent of correlation between all cation–anion pairs, that is, the sum of all individual cation–anion correlations, rather than the average correlation between any given ion pair.

**Computing Experimental Transport Properties from  $L^{ij}$ .** The Onsager transport coefficients may be combined to yield experimentally relevant transport properties, as summarized in Table 1. In addition to the self-diffusion coefficient discussed above capturing ideal Brownian motion, of particular interest is the ionic conductivity  $\sigma$ . Ionic conductivity is defined by using Ohm's law for a system with no concentration gradients; as such,  $\sigma$  gives a measure for how much current can be transported through an electrolyte for a given potential drop and is thus a crucial parameter for most energy storage applications. Experimentally,  $\sigma$  may be determined from AC impedance measurements.<sup>55</sup> For applications such as batteries with a single electroactive species (e.g., lithium ions), we care about not only the total conductivity but also the fraction of conductivity attributed to a given species. This is quantified by the transference number. In a lithium-ion battery, for example, it

is desirable for an electrolyte to exhibit a high cation transference number (close to unity) to avoid any significant current being carried by the inactive anion and the related formation of detrimental concentration gradients.<sup>16</sup> The transference number may be measured from techniques such as potentiostatic polarization,<sup>56,57</sup> the Hittorf method,<sup>58</sup> or electrophoretic NMR.<sup>59</sup> Finally, it is also useful to characterize the salt diffusion coefficient  $D_{\text{salt}}$  describing the relaxation of salt concentration gradients in an electrolyte (under no applied electric field), typically obtained experimentally from restricted diffusion measurements.<sup>60,61</sup> This quantity is defined by  $\frac{J_+}{\nu_+} = \frac{J_-}{\nu_-} = -D_{\text{salt}} \nabla c$ , where  $\nu_i$  is the stoichiometric coefficient of ion  $i$  in the salt. Unlike the other transport properties in Table 1,  $D_{\text{salt}}$  is not straightforward to compute from molecular dynamics, as it requires knowledge of the salt activity coefficient,  $f_{\text{salt}}$ . We provide expressions for each of these properties in terms of  $L^{ij}$  in Table 1 for the case of a binary electrolyte. These equations are readily generalized to multicomponent solutions, as provided by Fong et al.<sup>23</sup> We note that there exist Green–Kubo relations for computing some of these experimental properties directly, such as the conductivity.<sup>62,63</sup> These may be derived from the Green–Kubo relations for  $L^{ij}$  (eq 4) and the equations in Table 1. Additionally, we emphasize that the mappings from  $L^{ij}$  to experimental transport quantities are bidirectional: eqs 12, 14, and 16 may be rearranged to give the Onsager transport coefficients in terms of the experimentally measurable quantities  $\sigma$ ,  $t_+$ ,  $D_{\text{salt}}$ , and  $f_{\text{salt}}$ .

In addition to the aforementioned transport parameters, it is also common to report Nernst–Einstein (NE) transport quantities, which assume the solution behaves ideally with no correlations between species. Under this assumption, the off-diagonal terms of the transport matrix ( $L^{+-}$ ) and the distinct terms  $L_{\text{distinct}}^{ii}$  are equal to zero; thus, the diagonal transport coefficients may be related to the species' self-diffusion coefficients:  $L_{\text{NE}}^{ii} = L_{\text{self}}^{ii} = D_i c_i / RT$  (see eq 11). We present the ways in which the transport quantities change under this assumption in Table 1. While the NE assumption is only true in the limit of infinite dilution, it is nevertheless a useful approximation, as it requires much simpler experimental measurements than rigorously characterizing ion correla-

tions.<sup>17,57</sup> It is conventional to describe the deviation of the NE approximation by using the ionicity<sup>64–66</sup> (also called the inverse Haven ratio<sup>42,67,68</sup> or the degree of uncorrelated ion motion),<sup>69–71</sup> defined as the actual ionic conductivity divided by the NE conductivity ( $\sigma/\sigma^{\text{NE}}$ ). In the following sections, we will discuss certain circumstances in which the NE assumption fails substantially as well as instances in which the ionicity is a misleading metric for evaluating solution ideality.

**Comparing Onsager and Stefan–Maxwell Frameworks.** While the Onsager transport equations emerge naturally from the theory of nonequilibrium thermodynamics, they are not the dominant framework used by experimentalists to discuss transport. The most ubiquitous means of characterizing transport in concentrated solutions of both polymer and nonpolymer electrolytes is the Stefan–Maxwell equations, originally derived from the kinetic theory of gases:<sup>17–19,27</sup>

$$c_i \nabla \bar{\mu}_i = \sum_{j \neq i} K^{ij} (\mathbf{v}_j - \mathbf{v}_i) \quad (6)$$

where  $K^{ij}$  are the Stefan–Maxwell transport coefficients. These  $K^{ij}$  are commonly written in terms of the Stefan–Maxwell diffusion coefficients,  $\mathcal{D}^{ij}$ , as  $K^{ij} = \frac{RTc_i c_j}{c_T \mathcal{D}^{ij}}$ , where  $RT$  is the thermal energy and  $c_T$  is the total concentration (including solvent) of the electrolyte. Although the Stefan–Maxwell equations are more commonly used, we argue that the Onsager transport equations possess several advantages. Both frameworks can be used for continuum-level transport modeling<sup>72–75</sup> to predict concentration and potential profiles at a system level and can be used to obtain experimentally measurable quantities.<sup>17</sup> However, doing so is more challenging in the Stefan–Maxwell framework. Formulating the governing equations for macroscopic transport or writing expressions for experimentally measured properties relies on solving for the velocities of each species in solution; while this is trivial in the Onsager transport equations (eq 2), it requires extensive algebra in the Stefan–Maxwell equations (inverting the matrix of all  $K^{ij}$ ). This yields more complex expressions in the Stefan–Maxwell framework. The ionic conductivity, for example, can be written in terms of  $L^{ij}$  as a simple sum which easily generalizes to an arbitrary number of salt species:

$$\sigma = F^2 \sum_i \sum_j L^{ij} z_i z_j \quad (7)$$

In contrast, the conductivity of a binary salt in terms of  $\mathcal{D}^{ij}$  is<sup>17</sup>

$$\sigma = \left[ \frac{-RT}{c_T z_+ z_- F^2} \left( \frac{1}{\mathcal{D}^{+-}} - \frac{c_0 z_-}{c_+(z_+ \mathcal{D}^{0+} - z_- \mathcal{D}^{0-})} \right) \right]^{-1} \quad (8)$$

Generalizations to multicomponent solutions beyond a binary salt are much more involved and rarely reported.

Physically,  $K^{ij}$  may be interpreted as quantifying the friction between species  $i$  and  $j$ . For gaseous systems, this friction has a clear atomistic interpretation in terms of collisions between particles. The connection between  $K^{ij}$  and molecular-level motion in a liquid electrolyte, however, is more complex. Unlike  $L^{ij}$ , there is no Green–Kubo relation to directly compute  $K^{ij}$  from molecular dynamics simulations. Those works that do report Stefan–Maxwell coefficients from simulations do so by first computing the Onsager transport coefficients and then mapping from  $L^{ij}$  to  $K^{ij}$ .<sup>22,48,76,77</sup> For a binary electrolyte with a single solvent, this mapping, as derived in Fong et al.,<sup>23</sup> is

$$\begin{aligned} K^{+-} &= \omega_+ \omega_- \frac{\hat{L}^{00} + \hat{L}^{+-} - \hat{L}^{+0} - \hat{L}^{-0}}{\hat{L}^{+0} \hat{L}^{-0} - \hat{L}^{+-} \hat{L}^{00}} \\ K^{+0} &= \omega_+ \omega_0 \frac{\hat{L}^{--} + \hat{L}^{+0} - \hat{L}^{+-} - \hat{L}^{-0}}{\hat{L}^{+-} \hat{L}^{-0} - \hat{L}^{+0} \hat{L}^{--}} \\ K^{-0} &= \omega_- \omega_0 \frac{\hat{L}^{++} + \hat{L}^{-0} - \hat{L}^{+-} - \hat{L}^{+0}}{\hat{L}^{+-} \hat{L}^{+0} - \hat{L}^{-0} \hat{L}^{++}} \end{aligned} \quad (9)$$

where  $\hat{L}^{ik} = \frac{L^{ik}}{c_i c_k}$  and  $\omega_i$  is the mass fraction of species  $i$ .

Alternative methods for computing the Stefan–Maxwell coefficients directly have been proposed,<sup>78,79</sup> although their accuracy is somewhat contentious.<sup>22</sup> Thus, in summary, while both the Onsager and Stefan–Maxwell frameworks are correct,  $L^{ij}$  (i) yield simpler relations for experimentally relevant transport quantities than  $K^{ij}$ , (ii) are easier to compute from molecular simulations, and (iii) have a clearer physical interpretation, as they directly relate to ion correlations.

In the remainder of this Perspective, we discuss each of the various types of ion correlations that may exist in a polymer or polyionic electrolyte. We discuss the types of systems in which each type of correlation is expected to be most important using representative case studies from the literature. We provide insight into the molecular origins of these correlations, and where possible, we discuss how understanding each type of ion correlation can be used to inform the design of electrolytes with enhanced transport properties.

## ■ CATION–ANION CORRELATIONS

Understanding cation–anion correlations, captured in the transport coefficient  $L^{+-}$ , is crucial for the design of polymer-based electrolytes. As these correlations are induced by the inherent electrostatic attraction between cations and anions,  $L^{+-}$  will generally be non-negligible for most electrolytes used in energy storage applications, which typically employ moderately high concentrations and/or a relatively low dielectric constant. In general, an optimal polymer-based electrolyte will minimize cation–anion correlations, as a more positive value of  $L^{+-}$  will decrease the ionic conductivity of an electrolyte (eq 12), and for the common case where the cation transference number is less than one-half, a greater value of  $L^{+-}$  will also decrease  $t_+$  (eq 14).

In this section, we describe the molecular origins of cation–anion correlations in terms of both the structural features of the electrolyte as well as a dynamic picture of ion pair lifetimes, arguing that the latter is more useful in understanding trends in  $L^{+-}$ . We use this framework to guide a discussion on design rules for minimizing  $L^{+-}$  in polymer-based electrolytes. We conclude this section with a discussion of the special case of cation–anion correlations in two-component systems (free of solvent or host polymer), in which the theory dictates that cation and anion motion must be anticorrelated, with  $L^{+-} < 0$ .

**Static vs Dynamic Analyses of Ion Pairing.** Cation–anion correlations are conventionally discussed in terms of ion pairing or aggregation, that is, the fraction of ions that are bound to another ion at any given time.<sup>80</sup> In molecular simulations, it is common to use a distance criterion,<sup>29,81,82</sup> such as the first minimum of the radial distribution function, to define an ion as either free, paired, or part of a higher order aggregate such as a triple ion. This offers a computationally inexpensive means of characterizing ionic interactions in an electrolyte, as the

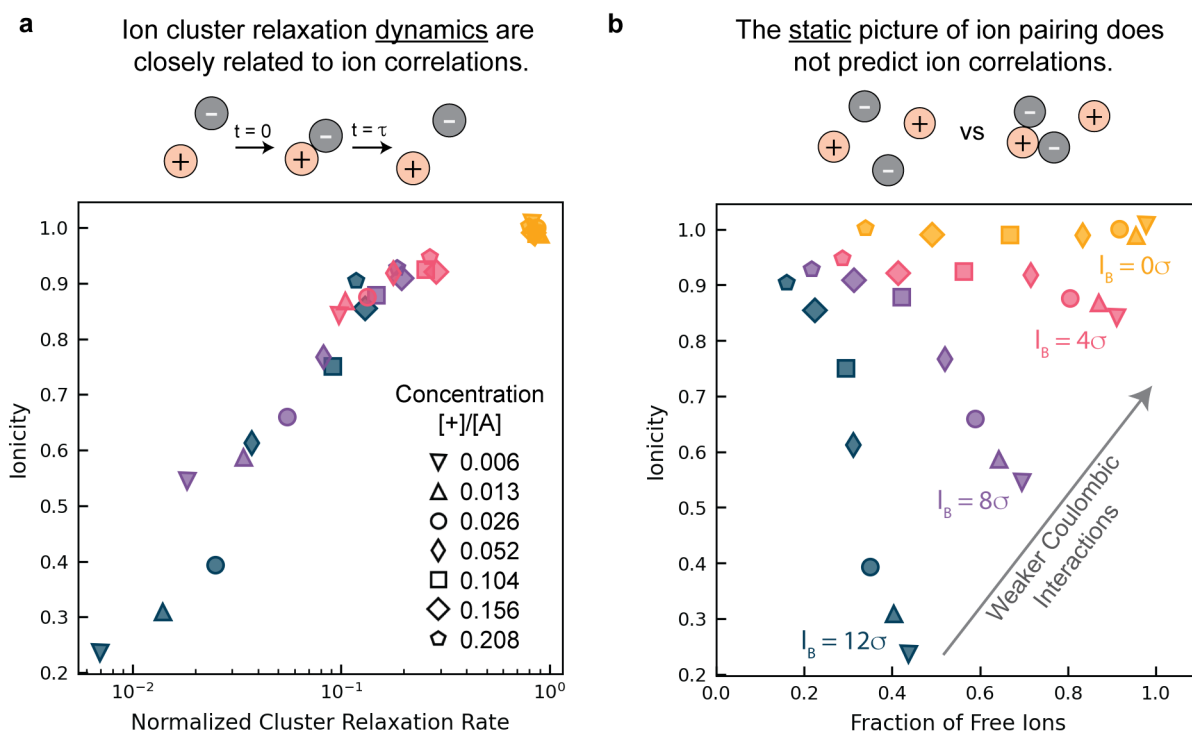


**Figure 3.** Demonstration that ion correlations in an electrolyte, as quantified by the ionicity, (a) correlate well with the relaxation time of ion clusters but (b) do not correlate well with the fraction of free ions determined from static structural analysis. Data are obtained from coarse-grained MD simulations of salt-doped homopolymers at varying concentration and Bjerrum length,  $l_B$ . Adapted with permission from ref 50.

simulation time scales of this ion pairing analysis are generally much shorter than those required for dynamic analyses.

In some systems, the static picture of ion pairing adequately captures cation–anion correlations, and we will use this framework throughout this text to intuitively rationalize trends in ion correlations. France-Lanord and Grossman<sup>83</sup> developed an effective method for computing ionic conductivity from molecular simulations which accounts for ion correlations exclusively through analysis of ion aggregates. Each aggregate is considered a distinct charge carrier, and its diffusion coefficient is used in the Nernst–Einstein equation to compute conductivity. This method gives reasonable agreement with the rigorously computed conductivity for LiTFSI in PEO. Burlatsky et al. used a simpler version of this approach for lithiated Nafion electrolytes containing nonaqueous solvents, in which the conductivity was estimated from the diffusion coefficient of only the free lithium ions and contributions from lithium ions paired to the Nafion polymer were ignored.<sup>84</sup> Furthermore, the static picture of ion pairing often forms the basis for theories of transport in polymer-based electrolytes, for example, by assuming that bound ions do not contribute to conductivity.<sup>85–87</sup> In the polyelectrolyte literature, the fraction of free ions is a key parameter in theories describing diffusion, including the presence of diffusion coefficients several orders of magnitude greater than expected from the Stokes–Einstein equation (called the “fast” mode).<sup>88–90</sup>

Despite the aforementioned utility of analyzing ion speciation to understand cation–anion correlations, a growing body of work suggests that this static picture alone is inadequate in many polymer-based electrolytes.<sup>91,92</sup> While the static picture analyzes the positions of the ions at a snapshot in time, the Green–Kubo relation for  $L^{+-}$  requires integrating the flux–flux correlation function over time, suggesting that a dynamic (time-dependent)

analysis is necessary to understand how cation–anion interactions affect experimentally observable transport properties. The static ion pairing definition will generally overestimate cation–anion correlations: an ion pair that breaks apart immediately after forming, for example, will be accounted for in the static picture of ion pairing but will not contribute significantly to  $L^{+-}$ . Likewise, ions that hop directly between charged sites of a polyion (without first traveling through the surrounding dielectric medium) will contribute to the conductivity despite the fact that the ions remain continuously paired. This type of ion transport has been observed as a crucial mechanism in a variety of systems, including polyelectrolytes,<sup>29,93</sup> polymerized ionic liquids,<sup>94</sup> and ionomer melts.<sup>52,95–97</sup> The potential limitations of the static picture to describe cation–anion correlations have important implications for the interpretation of the ionicity ( $\sigma/\sigma^{\text{NE}}$ , eq 18) as well. It is often assumed that the ionicity corresponds to the fraction of free ions in the system, that is, that the extent of ion correlation in an electrolyte is given directly by the degree of ion pairing.<sup>98,99</sup> While there are some works in which the ionicity does indeed agree well with the fraction of free ions computed from molecular dynamics, for example, in Borodin and Smith’s simulations of LiTFSI in PEO,<sup>100</sup> in what follows we discuss several instances in which this is not the case. As an extreme example, the ionicity of (polymerized) ionic liquids is often comparable to that of conventional liquid electrolytes;<sup>69–71,101–103</sup> it is well-established that the static picture of ions as either bound or free fails for superconcentrated systems such as these.<sup>104–106</sup>

Beyond the static fraction of ion pairing, further insight into cation–anion correlations can be obtained by analyzing the residence time of ion pairs,  $\tau$ , or the average time that an ion pair persists before breaking apart. In molecular dynamics

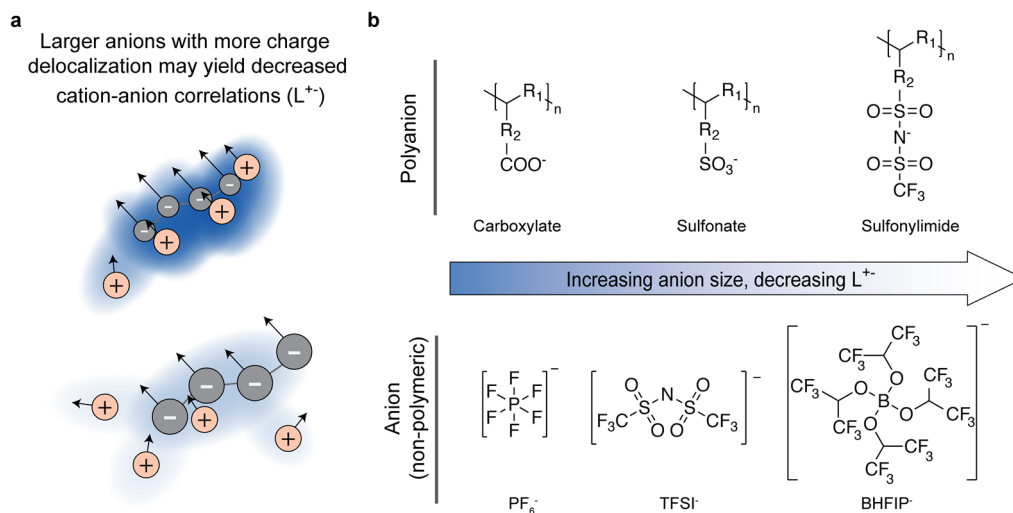


**Figure 4.** (a) Illustration of the weaker ion correlations expected in systems employing larger ions with greater charge delocalization. Correlations are colored according to the color bar in Figure 2. (b) Examples of common chemistries employed to increase anion charge delocalization in polyanions (top) and small-molecule anions (bottom).

simulations,  $\tau$  may be computed based on the autocorrelation function  $P_{\alpha\beta}(t) = \langle H_{\alpha\beta}(t)H_{\alpha\beta}(0) \rangle$ , where  $H_{\alpha\beta}(t)$  equals one if particles  $\alpha$  and  $\beta$  are neighbors at time  $t$  and zero otherwise. The decay time of  $P_{\alpha\beta}(t)$ , defined by either a stretched exponential fit or simply the time for the function to reach a certain value, yields  $\tau$ .<sup>29,50,96,107–109</sup>

Analysis of ion pair or cluster residence times has been shown to yield excellent correlation with the extent of ion correlations in an electrolyte. Shen and Hall,<sup>50</sup> for example, compared the ionicity in salt-doped homopolymers and block copolymers with both the static fraction of ion pairs and the normalized cluster relaxation rate (defined as the inverse residence time of an ion cluster divided by the polymer relaxation rate) using coarse-grained MD simulations. Assuming that cation–cation and anion–anion interactions do not dominate transport in these systems of neutral polymer electrolytes, the ionicity provides indirect insight into  $L^{+-}$ . For a range of Coulomb strengths, the authors found that the normalized cluster relaxation rate correlated directly with the ionicity (Figure 3a), while the fraction of free ions obtained from structural analysis was found to be anticorrelated to ionicity, as shown in Figure 3b. This stands in direct contrast with the common interpretation of the ionicity as the fraction of free ions described above. The phenomenon of  $L^{+-}$  correlating with ion dynamics rather than statics has been demonstrated in polyelectrolyte solutions as well. Our previous work on transport in short-chain polyelectrolyte solutions, using both atomistic<sup>29</sup> and coarse-grained<sup>50</sup> molecular dynamics, showed that changes in the contribution to  $L^{+-}$  per ion could not be rationalized by trends in the static fraction of ion pairs but rather paralleled the trends in ion pair residence times. In both Shen and Hall's solid polymers and the aforementioned polyelectrolyte solutions, cation–anion correlations (and correspondingly ion pair residence times) decrease as the concentration increases, despite the fact that ion pairing from the static picture increases with concentration. Experimental measurements have similarly reported increasing ionicity as concentration increases, that is, less correlated ion motion at high concentrations.<sup>45,110,111</sup> This decrease in cation–anion correlations at high concentrations warrants further exploration, but it may be due to a shift in transport mechanisms or solvation environments and/or the fact

all mass fluxes must sum to zero in the system, which place constraints on the relative values of the transport coefficients.

**Design Principles for Minimizing Cation–Anion Correlations.** Design of electrolytes with high ionic conductivity should aim to minimize cation–anion correlations. The simplest means of tuning the value of  $L^{+-}$  is to alter the charge density of the electrolyte ions. To this end, several recent computational works have investigated the effect of altering ionic size and/or ion dipole strength on ion transport.<sup>96,112–116</sup> Cheng et al.,<sup>112</sup> for example, suggested that optimal conductivity in polymerized ionic liquids could be obtained by using large ions in the polymer chain and small counterions. Using both coarse-grained and atomistic MD simulations, they found that this design choice led to optimal decoupling of ion motion and segmental dynamics. Molinari et al.<sup>114</sup> altered the charge density of TFSI<sup>-</sup> anions in MD simulations of LiTFSI in PEO by scaling the anion partial charges, finding that a more polar anion decreased Li<sup>+</sup> mobility and increased ion clustering, while an anion with a more uniform charge distribution had the opposite effect. This trend that increasing anion charge delocalization improves transport, specifically via a decrease in  $L^{+-}$ , is a general design rule that holds across many systems (Figure 4a).

Common chemistries used to enhance anion charge delocalization are presented in Figure 4b. In solid polymer electrolytes, anions such as PF<sub>6</sub><sup>-</sup> and TFSI<sup>-</sup> are some of the most commonly studied.<sup>112</sup> It has been experimentally demonstrated in carbonate solvents<sup>117</sup> that TFSI<sup>-</sup> has a smaller thermodynamic ion association constant than PF<sub>6</sub><sup>-</sup> and that TFSI<sup>-</sup> exhibits higher  $t_+$  in polymer-based electrolytes.<sup>118</sup> It is worth noting that recent studies on multivalent (nonpolymeric) electrolytes for energy storage applications have also worked toward lowering cation–anion interaction via increased anion charge delocalization. One notable example is the fluorinated alkoxyborate BHFIP<sup>-</sup> anion, which allows for reduced ion pairing and thus improved transport because of its large size.<sup>119–122</sup> Polyanionic single-ion conductors often employ sulfonylimide groups (analogous to the chemistry of a TFSI<sup>-</sup> anion), which provide more charge delocalization than sulfonate or carboxylate moieties. The greater charge delocalization in these anions has been shown to correlate with higher conductivity in a variety of systems.<sup>123–126</sup> For advances in



synthesis strategies and further examples of successful single-ion conductor chemistries, we refer the reader to the recent review by Zhang et al.<sup>15</sup>

While the trend of decreased cation–anion correlation with greater anion charge delocalization holds for many systems, in some cases changes in the charge distribution of an ion can alter the transport mechanisms in an electrolyte, complicating the resulting changes in bulk transport. This has been observed in the MD simulations performed by Lin and Maranas<sup>115</sup> of PEO-based single ion conducting solid polymer electrolytes. Here, the cation–anion electrostatic interactions were tuned by changing the partial charges of the sulfonate anion appended to the polymer backbone. As expected, a more charge-delocalized anion (weaker electrostatic interactions) decreased ion aggregation. While one would intuitively expect this decreased aggregation to yield increased conductivity, it was observed that the mobility of the sodium cation in the system remained unchanged. The authors attribute this counterintuitive result to a changing diffusion mechanism: with weak electrostatic interactions, motion was dominated by free ions solvated by the EO backbone, whereas with stronger electrostatic interactions, hopping of the cation between sulfonate anions became the dominant process. In the work of Ma et al. reporting coarse-grained MD simulations of random ionomer melts,<sup>96</sup> modifying the cation/anion size ratio resulted in substantial changes to both nanostructure and ion pair residence times. Depending on the dielectric constant and applied electric field, these changes in ion size sometimes increased and sometimes decreased cation mobility. Furthermore, we note that the impact of altering charge delocalization of the cation is often more complex than changing that of the anion, namely in solid polymer electrolytes where the cation and polymer host strongly interact. A larger cation has been shown to enhance transport in some cases<sup>113,127</sup> by minimizing cation–anion correlation, whereas in other cases the presence of free cations can mediate cross-linking of polymer chains and lead to reduced mobility.<sup>128</sup>

**$L^{+-}$  in Polymerized Ionic Liquids.** Finally, we note that when analyzing  $L^{+-}$ , special care must be taken for the case of two-component systems such as polymerized ionic liquids with only a single type of cation, a single type of anion, and no additional solvent or polymer host. As mentioned in the Theory section, an  $n$ -component system will possess  $n(n - 1)/2$  independent transport coefficients. Thus, for a two-component system, only one transport coefficient can be independently specified. The others may be computed from the constraint  $\sum_i M_i L^i = 0$  obtained as a consequence of the barycentric reference frame:  $L^{--} = \frac{M_+^2}{M_-^2} L^{++}$  and  $L^{+-} = -\frac{M_+}{M_-} L^{++}$ . Thus,  $L^{+-}$  must always be *negative* in these systems.<sup>30,129</sup> Mathematically, the Green–Kubo relation for  $L^{+-}$  (eq 4) suggests that a negative value corresponds to anticorrelated cation–anion motion. However, because the relative motion of the cation and anion is constrained and  $L^{+-}$  is not an independent quantity in two-component systems,  $L^{+-}$  does not give straightforward insight into cation–anion interactions in these electrolytes. Furthermore, the behavior and interpretation of the transference number in these cases are nonintuitive. Based on eq 14 and the aforementioned constraints in  $L^j$ , the cation transference number in a two-component system is dictated solely by the charge valences and molar masses of the ionic species:

$$t_+ = \frac{z_+ M_-}{z_+ M_- - z_- M_+} \quad (20)$$

This yields the surprising result that transference number is independent of chain length in polymerized ionic liquids.<sup>30,42</sup> In the limit where the anion mass is much larger than that of the cation (as is usually the case for polymer-based single ion conductors),  $t_+$  approaches unity, as is typically reported experimentally for these systems.<sup>130–133</sup> We note, however, that in these two-component electrolytes the transference number is not meaningful as an electrolyte performance metric. The transference number is typically used to predict the extent to which detrimental concentration gradients will form in an electrochemical cell.<sup>16,134</sup> In a two-component system, however, electroneutrality dictates that no concentration gradients will form, regardless of the value of the transference number given by eq 20. In these systems the ionic conductivity will be the only independent property impacting bulk transport.

## ■ CATION–CATION AND ANION–ANION CORRELATIONS

In nonpolymeric liquid electrolytes, particularly those that are dilute, cation–cation and anion–anion correlations ( $L_{\text{distinct}}^{++}$  and  $L_{\text{distinct}}^{--}$ ) are not expected to contribute substantially to electrolyte transport. It is anticipated that like ions will either interact very little or move in an anticorrelated manner because of electrostatic repulsion, yielding negative values of  $L_{\text{distinct}}^{ii}$  with small magnitude.<sup>30,34</sup> In polymer-based electrolytes, however,  $L_{\text{distinct}}^{ii}$  may contribute substantially. This contribution is most notable in (i) polyionic systems, where the covalent links between charged monomers create strong correlations between charges on a given chain, and (ii) systems with substantial ion aggregation such as low-permittivity polymer electrolytes. We address both cases in this section.

### Polyions Generate Strong Like-Ion Correlations.

Covalent attachment of multiple ions to yield a polyion inevitably introduces strong like-ion correlations. For oligomeric polyions, all ions on a given chain are constrained to move together; that is, over sufficiently long time scales the flux of any given monomer on a chain will be equal to that of the chain center-of-mass. For longer chains or systems with very slow dynamics, distinct monomers may not be perfectly correlated over the time scale of a simulation (or experiment), but substantial correlation will nevertheless exist between ions on nearby monomers. Our group's MD simulations of anionic polyelectrolytes<sup>29,30</sup> found that in many systems  $L_{\text{distinct}}^{--}$  is the largest of all the transport coefficients. As these correlations are induced by the covalent bonding of the ions, this substantial contribution of  $L_{\text{distinct}}^{--}$  is expected for anionic polyelectrolytes regardless of the specific chain chemistry or solvent properties. Note that, in addition to correlations between anions attached to the same polymer chain (which yield large, positive contributions to  $L_{\text{distinct}}^{--}$ ), we also expect correlations between anions on different chains. These correlations may be negative because of electrostatic repulsion between like charges, or under some conditions, there may be positive correlation from aggregation of like-charge chains. This aggregation may be induced by dipoles and/or quadrupoles formed from charged monomers and adsorbed counterions; this phenomenon is thought to give rise to the “slow” (extraordinary) diffusion coefficient observed in dynamic light scattering experiments on salt-free polyelectrolyte solutions.<sup>88,89,135,136</sup> While the relative magnitude of anion correlations within and between chains will be system-dependent, we have found that contributions from intrachain correlations typically dominate those from interchain correlations, resulting in the observed positive values of  $L_{\text{distinct}}^{--}$ .

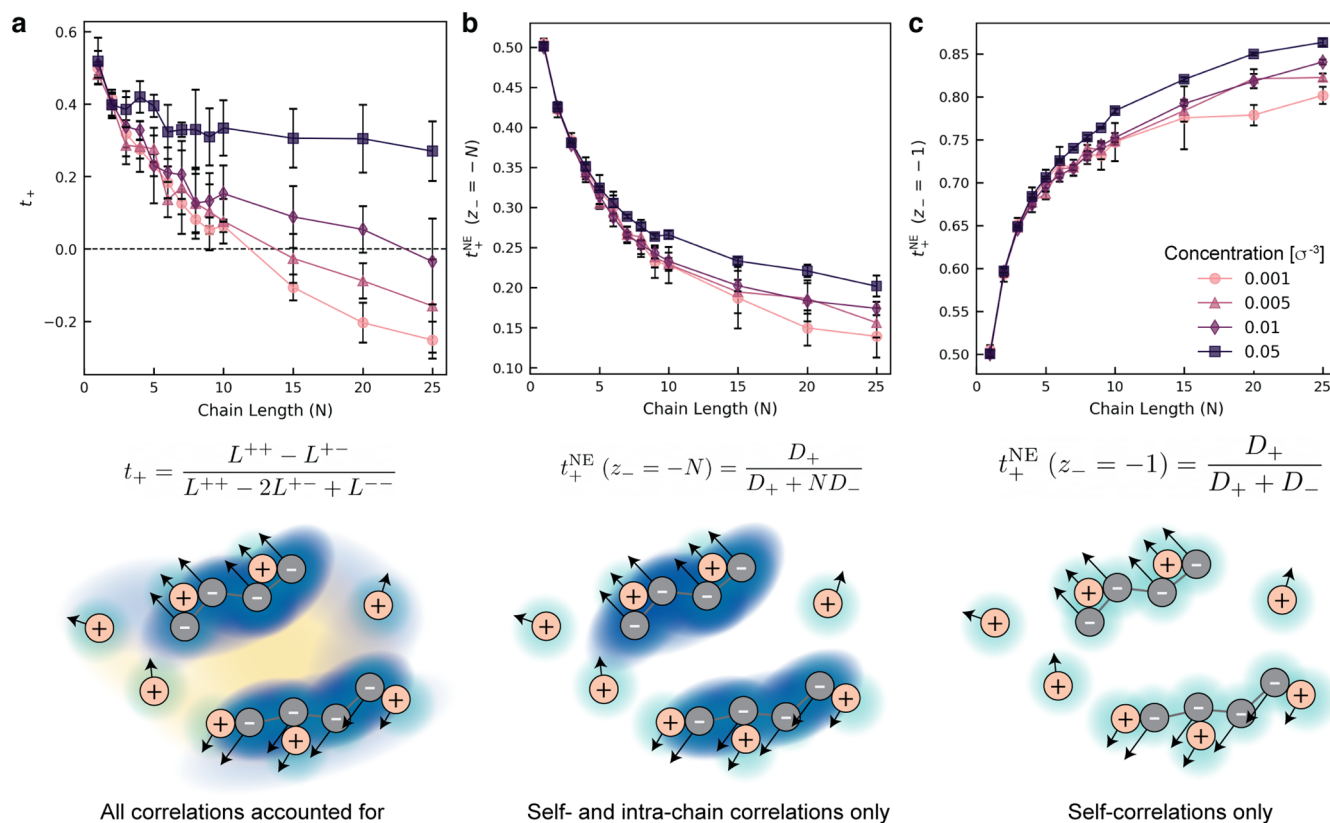


**Figure 5.** Cation transference numbers computed from coarse-grained MD simulations of anionic polyelectrolyte solutions. (a) Rigorously computed transference number accounting for all ion correlations. (b, c) Transference numbers employing ideal solution (Nernst–Einstein) approximations. The equation used to generate the data in (c) ignores all correlations between ions and is in line with common experimental approximations. The approximation in (b) captures correlations between anions within the same chain and yields a more reasonable estimate of the true  $t_+$ . Reproduced with permission from ref 30.

As a result of the large magnitude of  $L_{\text{distinct}}^{--}$  in polyionic solutions, the Nernst–Einstein approximation (which assumes all  $L_{\text{distinct}}^i$  and  $L^{+-}$  are zero) fails drastically for these systems. Several recent experimental works, however, have used the Nernst–Einstein assumption to characterize the transference number in nonaqueous polyionic systems for application in lithium-ion batteries<sup>98,103,137,138</sup> using  $t_+^{\text{NE}} = \frac{D_+}{D_+ + D_-}$ . As the self-diffusion coefficient of the anion is much smaller than that of the counterion in these systems, the  $t_+^{\text{NE}}$  approximation typically yields very high cation transference numbers ( $t_+^{\text{NE}} > 0.8$ , compared to  $t_+ \approx 0.4$  for conventional liquid electrolytes). We have found,<sup>29,30</sup> however, that the true transference number incorporating ion correlations (which is the relevant quantity in predicting macroscopic concentration profiles and electrolyte performance) is drastically lower. As shown in Figure 5a,c for coarse-grained MD simulations of polyelectrolytes at various concentrations and chain lengths,  $t_+^{\text{NE}}$  does not even qualitatively reproduce the trend in the rigorously computed  $t_+$  because of the large values of  $L_{\text{distinct}}^{--}$  and  $L^{+-}$  in these systems. Note that the above discussion of  $L_{\text{distinct}}^{--}$  has considered the anionic species to be individual charged monomers, as opposed to taking the anionic species to be the polymer chain as a whole. While either approach is valid and gives the same conductivity and transference number,<sup>30</sup> the two choices yield different Nernst–Einstein transference numbers. Considering each monomer separately (the approach commonly used to characterize nonaqueous polyionic electrolytes experimentally)<sup>98,103,137,138</sup> does not yield physically meaningful insight

into transport, as it incorrectly assumes that covalently bound anions move completely independently from one another; conversely, considering the entire chain together (as in Figure 5b) implicitly captures intrachain correlations and gives a much more reasonable estimate of the true  $t_+$ . Importantly, for these polyionic solutions, incomplete characterization of ion correlations can lead to an incorrect understanding of ion transport—based on ideal solution (Nernst–Einstein) assumptions treating each charged monomer as an independent ion, these polyelectrolyte solutions seem like promising alternatives to conventional battery electrolytes, whereas in actuality their transport properties are substantially less favorable than standard electrolyte formulations.

The behavior of  $L_{\text{distinct}}^i$  in two-component (solvent-free) systems such as polymerized ionic liquids is more complex, as the transport coefficients in these systems must satisfy the constraint  $\sum_i M_i L^i = 0$ . Zhang et al.<sup>42</sup> performed atomistic MD simulations of polycationic polymerized ionic liquids and observed anticorrelated cation–cation motion, despite the fact that cations on a given chain were covalently constrained to move together. Our group’s coarse-grained simulations of polymerized ionic liquids, however, reported the opposite trend (positively correlated anion–anion motion for a negatively charged polymer).<sup>30</sup> We recommend further studies to reconcile the origin of these differences.

**Strongly Aggregating Systems: The Questions of Near-Unity Ionicity and Negative Transference Numbers.** Distinct anion–anion or cation–cation correlations

( $L_{\text{distinct}}^i$ ) are also expected to be substantial in systems with low dielectric constant that have a high degree of ion aggregation, where ions of the same type in a given aggregate will move together in a correlated manner for the lifetime of the aggregate. Ion aggregation will simultaneously increase both cation–anion correlations ( $L^{+-}$ ) and like-ion correlations ( $L_{\text{distinct}}^i$ ). While the former decreases the ionic conductivity, the latter will increase it. Thus, the effect of ion aggregation on bulk conductivity may not be apparent a priori. Generally, aggregation is associated with slower dynamics and the formation of neutral clusters which do not contribute to conductivity:<sup>80</sup> in a long-lived, charge-neutral aggregate, the contributions of  $L^{+-}$  and  $L_{\text{distinct}}^i$  to the overall conductivity should cancel out. In the case of charged aggregates or systems with frequent exchange/rearrangement of aggregate populations, however, strong aggregation may actually enhance conductivity. In some cases, extensive aggregation leads to the formation of percolating networks which yield facile ion transport, as observed in ionomers<sup>52,97,139–141</sup> and polymerized ionic liquids.<sup>112</sup>

Because of the complex interplay of cation–anion, cation–cation, and anion–anion correlations, we could envision a system with very strong ion correlations that possesses ionicity close to unity due to the cancellation of contributions from  $L^{+-}$  and  $L_{\text{distinct}}^i$ .<sup>129</sup> Care should thus be taken when interpreting the ionicity as the degree of ideal or uncorrelated transport in an electrolyte. Large  $L_{\text{distinct}}^i$  may rationalize experimental<sup>100,142–144</sup> and computational<sup>145,146</sup> observations of relatively high ionicity in solid polymer electrolytes. As we are not aware of any works that have explicitly computed  $L_{\text{distinct}}^i$  in these systems, quantification of the extent to which these correlations dictate ionicity and other bulk transport properties remains an interesting avenue for further study.

We also note that like-ion correlations ( $L_{\text{distinct}}^i$ ) and ion aggregation may be used to rationalize the phenomena of negative cation transference numbers, which have been measured experimentally<sup>147</sup> and from MD simulations<sup>83</sup> in PEO-based electrolytes. Qualitatively, negative transference numbers may be rationalized through the presence of negatively charged aggregates. Recall that the transference number is the fraction of conductivity attributed to a given species, which we may write by using a ratio of electrophoretic mobilities:  $t_i = Fz_i c_i u_i / (\sum_j Fz_j c_j u_j)$ , where the electrophoretic mobility is defined as  $u_i = (v_i - v)/E$ . In general, we expect an anion to move toward more positive potential, corresponding to a negative mobility, and a cation to move toward more negative potential (positive mobility), such that the quantity  $z_i u_i$  and thus the transference number are generally positive. Consider, however, a cation which is part of a net-negative aggregate such as a triple ion with two anions and one cation. The aggregate as a whole will move toward more positive potential, so the cation in the aggregate will migrate in the “wrong” direction and have negative mobility.<sup>148</sup> As the total cation mobility is an average over all cations in the system, the overall average cation mobility can be negative (yielding a negative cation transference number) if enough cations are part of negatively charged aggregates and if the mobility of those aggregates is sufficiently large. Mathematically,  $t_+ < 0$  corresponds to a system where  $L^{+-} > L^{++}$  (eq 14). This is also consistent with the presence of negatively charged aggregates, where  $L_{\text{distinct}}^{+-}$  is small relative to  $L^{+-}$  and  $L_{\text{distinct}}^{--}$ . Although there remains some uncertainty based on measurement technique as to whether PEO-based electrolytes actually have negative  $t_+$ ,<sup>110</sup> molecular simulations in PEO-based electrolytes have in certain circumstances observed negatively

charged aggregates.<sup>114,149</sup> Negative cation transference numbers have been observed through simulation<sup>30</sup> and experiment<sup>150–154</sup> in anionic polyelectrolyte solutions as well, where negatively charged aggregates are common (for example, a single cation bound to a polyanion chain).

## ION–SOLVENT CORRELATIONS

Bulk transport properties such as the conductivity and transference number are computed by using only  $L^{++}$ ,  $L^{--}$ , and  $L^{+-}$ . Transport coefficients for the solvent or polymer host ( $L^{+0}$ ,  $L^{-0}$ , and  $L^{00}$ ) are not only unnecessary to compute these quantities, but for a binary, single-solvent electrolyte they also can be computed directly from knowledge of  $L^{++}$ ,  $L^{--}$ , and  $L^{+-}$ ; that is, they are not independent quantities. Using the aforementioned constraint  $\sum_j M_j L^j = 0$ , we can write the solvent transport coefficients of a binary electrolyte as

$$\begin{aligned} L^{+0} &= -\frac{1}{M_0}(M_+ L^{++} + M_- L^{+-}) \\ L^{-0} &= -\frac{1}{M_0}(M_+ L^{+-} + M_- L^{--}) \\ L^{00} &= -\frac{1}{M_0}(M_+ L^{+0} + M_- L^{-0}) \end{aligned} \quad (21)$$

Note that because  $L^{++}$ ,  $L^{--}$ , and  $L^{+-}$  are generally positive, eq 21 implies that  $L^{+0}$  and  $L^{-0}$  will be negative (anticorrelated motion), while  $L^{00}$  will be positive. Although the solvent transport coefficients are not directly useful in obtaining experimentally relevant transport properties, tuning ion–solvent interactions can have a substantial impact on  $L^{++}$ ,  $L^{--}$ , and  $L^{+-}$ . Increasing cation–solvent correlation (making  $L^{+0}$  less negative), for example, would correspond to decreasing  $L^{++}$  (slower cation self-diffusion) and/or  $L^{+-}$  (weaker cation–anion correlations). In this section, we explore how changing various aspects of ion–solvent interactions affects the ion correlations discussed in the previous sections as well as how these modifications affect bulk transport properties.

One of the key solvent properties dictating correlations in an electrolyte is the dielectric constant  $\epsilon$ . As would be expected from Coulomb’s law, increasing the dielectric constant generally decreases cation–anion correlations  $L^{+-}$ . In solid polymer electrolytes, it has been observed by using both atomistic<sup>155</sup> and coarse-grained<sup>50,116,145,146</sup> MD that a greater dielectric constant or polymer polarity increases ionicity and decreases ion aggregation. Similarly, in simulations of random ionomer melts, Ma et al.<sup>96</sup> observed shorter cation–anion residence times and higher ion mobility with higher dielectric constant. While the decreases in  $L^{+-}$  induced by higher dielectric constant will favor higher overall ionic conductivity, several works have demonstrated nonmonotonic trends in ion transport with respect to dielectric constant. This trend is clearly illustrated in the coarse-grained MD simulations of solid polymer electrolytes performed by Wheatle et al.,<sup>145</sup> as shown in Figure 6. At low polymer polarity, ionicity data suggest that conductivity may be limited by high  $L^{+-}$  as a result of ion aggregation. At high polarity, however, the ionicity remains high but transport is limited by polymer segmental dynamics. The latter is expected to decrease self-diffusion of ions, especially that of the cation ( $L_{\text{self}}^{++}$ ) due to the strong coupling of cation diffusion and polymer dynamics in most solid polymer electrolytes.<sup>100,114</sup> Note that the overall dielectric constant of the solution in these simulations may also be affected by the polarity of ionic clusters

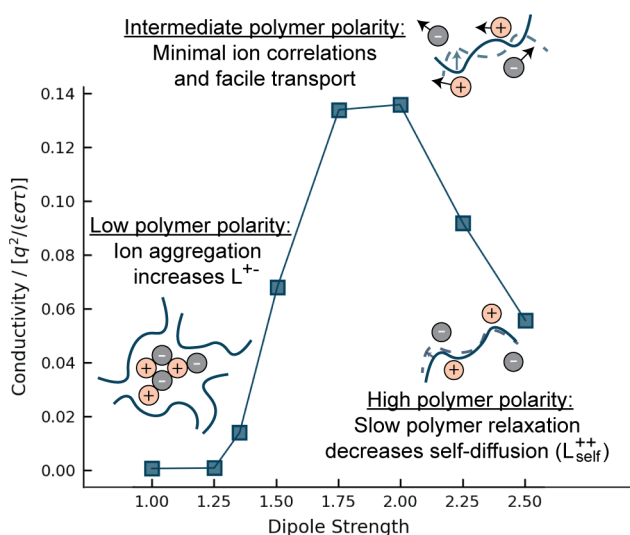


**Figure 6.** Ionic conductivity as a function of host polymer dipole strength obtained from coarse-grained molecular dynamics simulations of salt-doped solid polymer electrolytes. Adapted with permission from ref 145.

(in addition to the polarity of the polymer itself), which has been found to significantly affect the dielectric constant of PEO-based electrolytes in experimental studies.<sup>144,156,157</sup> The trade-off between polymer segmental motion and dielectric constant has also been observed experimentally, for example, by Choi et al. in polysiloxane-based single-ion conductors, where maximal conductivity was observed by using plasticizers with intermediate glass transition temperature and dielectric constant.<sup>158</sup> Others have similarly observed that ion transport is optimized at intermediate dielectric constant but attributed the trend to changes in the ion transport mechanism with respect to  $\epsilon$ . Gudla et al.<sup>159</sup> have found that the polymer dielectric constant (tuned by scaling partial charges in atomistic MD) has a substantial impact on transport in LiTFSI–PEO. They suggest that as dielectric constant increases,  $\text{Li}^+$  motion transitions from vehicular diffusion to primarily interchain hopping and then ultimately to intrachain hopping, with the interchain hopping at intermediate  $\epsilon$  yielding the fastest lithium diffusion. In ionomer melts, Bollinger et al.<sup>97</sup> have suggested that optimal conductivity can be reached when Coulombic interactions are strong enough to allow for a percolated aggregate structure but weak enough to favor ion dissociation and short residence times.

In addition to tuning bulk solution properties such as the dielectric constant, transport in polymer-based electrolytes may also be tuned via solvent/polymer chemistry, which alters short-range interactions between species. Computational methods are particularly well-suited to evaluating these effects, as they allow for precise control of chemical structure in materials that may be difficult to synthesize experimentally. In solid polymer electrolytes where strong cation–polymer interactions typically dictate transport,<sup>100,114,160</sup> several works have explored the strategy of increasing polymer–anion interactions ( $L^{-0}$ ) to improve transport properties. Savoie et al.,<sup>51</sup> for example, simulated Lewis acidic polymers (polyboranes) which preferentially coordinated with the anionic species, observing substantial decreases in anion diffusion ( $L_{self}^{-}$ ) and increases in cation diffusion ( $L_{self}^{+}$ ). Similarly, France-Lanord et al.<sup>149</sup> used classical MD to investigate a PEO variant with sulfonyl secondary sites, finding that the strong interaction between the sulfonyl group

and the anion ( $\text{TFSI}^-$ ) preferentially decreased anion transport and led to increased lithium ion transference number. These authors also studied the effect of carbonate secondary sites on the polymer chain, which increased polymer–cation interactions. In this carbonate-containing system, the increase in  $L^{+0}$  presumably decreased  $L^{+-}$ , as a substantial reduction in ion pairing was observed. Note that it may be impractical to attempt to tune polymer–ion interactions without inadvertently affecting ion transport mechanisms. In PEO, it is understood that lithium ions move through a well-connected network of solvation sites which promote facile intrachain hopping.<sup>54</sup> Alternate polymer structures may not be conducive to this mechanism. Classical MD simulations of polyester-based polymer electrolytes, for example, found mainly isolated clusters of polymer solvation sites, in which the main transport mechanisms were infrequent interchain hopping and codiffusion with the polymer chain. These slower processes yielded ionic conductivities an order of magnitude lower than in PEO.<sup>54</sup>

## CONCLUSIONS AND RECOMMENDATIONS

Ion correlations play a crucial role in the transport properties of polyionic and polymer electrolytes. The Onsager transport equations and corresponding transport coefficients  $L^j$  are an underutilized framework for rigorously quantifying these ion correlations. In contrast to the more widely known Stefan–Maxwell coefficients,  $L^j$  can be computed easily from molecular dynamics simulations by using ions' positions or velocities; our code to perform this calculation is freely available at <https://github.com/kdfong/transport-coefficients-MSD>.

In this Perspective, we have discussed how cation–anion, like-ion, and ion–solvent correlations impact transport in polymer-based electrolytes. We demonstrate the limitations of some of the conventional paradigms for analyzing ion correlations, for example, by using the static fraction of ion pairing as a proxy for cation–anion correlations and applying the Nernst–Einstein approximation to polyionic systems. Several design rules are suggested from our analysis, namely, the use of ions with highly delocalized charge to decrease cation–anion correlations as well as use of a solvent or polymer host with an intermediate value of dielectric constant to balance trade-offs between ion aggregation and self-diffusion.

We recommend that calculation of  $L^j$  should become standard practice in characterization of electrolyte transport. There are several systems for which we anticipate insight into transport coefficients and ion correlations from molecular dynamics simulations will be particularly valuable at addressing long-standing questions in the field. Of note are PEO-based electrolytes for lithium-ion batteries, where experimental studies have demonstrated a variety of complex transport phenomena such as negative cation transference number and diverging Stefan–Maxwell diffusion coefficients.<sup>20,147</sup> Knowledge of  $L^j$  could elucidate the molecular origins of these phenomena, which are still under debate. Additional attention should also be devoted to the study of  $L^j$  in two-component systems such as polymerized ionic liquids, where the transport coefficients are all interdependent as a consequence of the barycentric reference frame. The counterintuitive relationships between  $L^{+-}$ ,  $L_{self}^i$  and  $L_{distinct}^i$  in these systems are still poorly understood, particularly with regards to the effect of changing chain length, dielectric constant, and ion chemistry. Furthermore, the Onsager transport framework is well-suited to treat multicomponent systems with more than one type of cation and/or anion, such as the complex solutions handled in the fields of biology,

geochemistry, and water purification.<sup>8,9</sup> We also note the widespread use of supporting electrolytes<sup>161</sup> in energy storage applications.

Finally, we emphasize that the adoption of the Onsager transport framework is not exclusive to molecular simulations. Just as we can compute experimentally measurable transport quantities from knowledge of  $L^j$  by using the equations in Table 1, we may also compute  $L^j$  from experimentally measured quantities such as conductivity, transference number, and salt diffusion coefficient.<sup>23</sup> The Onsager transport coefficients can serve as a powerful means of connecting observations from experiment and simulation. We believe this approach has the potential to enable both enhanced fundamental understanding and more rational design of polymer-based electrolytes.

## AUTHOR INFORMATION

### Corresponding Author

**Kristin A. Persson** – Department of Materials Science and Engineering, University of California, Berkeley, Berkeley, California 94720, United States; The Molecular Foundry, Lawrence Berkeley National Laboratory, Berkeley, California 94720, United States; [orcid.org/0000-0003-2495-5509](https://orcid.org/0000-0003-2495-5509); Email: [kapersson@lbl.gov](mailto:kapersson@lbl.gov)

### Authors

**Kara D. Fong** – Department of Chemical and Biomolecular Engineering, University of California, Berkeley, Berkeley, California 94720, United States; Energy Technologies Area, Lawrence Berkeley National Laboratory, Berkeley, California 94720, United States; [orcid.org/0000-0002-0711-097X](https://orcid.org/0000-0002-0711-097X)

**Julian Self** – Energy Technologies Area, Lawrence Berkeley National Laboratory, Berkeley, California 94720, United States; Department of Materials Science and Engineering, University of California, Berkeley, Berkeley, California 94720, United States

**Bryan D. McCloskey** – Department of Chemical and Biomolecular Engineering, University of California, Berkeley, Berkeley, California 94720, United States; Energy Technologies Area, Lawrence Berkeley National Laboratory, Berkeley, California 94720, United States; [orcid.org/0000-0001-6599-2336](https://orcid.org/0000-0001-6599-2336)

Complete contact information is available at:

<https://pubs.acs.org/10.1021/acs.macromol.0c02545>

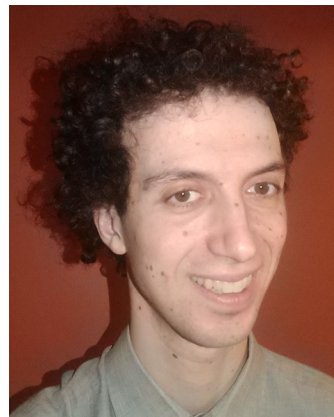
### Notes

The authors declare no competing financial interest.

### Biographies



Kara Fong is a Ph.D. candidate in the Department of Chemical & Biomolecular Engineering at the University of California, Berkeley, coadvised by Prof. Bryan McCloskey and Prof. Kristin Persson. She completed her master's degree at the University of Cambridge and her bachelor's degree at Stanford University. Her current research focuses on understanding transport phenomena in electrolyte solutions for Li-ion batteries using molecular dynamics simulations and nonequilibrium thermodynamics.



Julian Self is a Ph.D. candidate in the department of Materials Science and Engineering at the University of California, Berkeley, working in Kristin Persson's group. He previously received a M.Sc. from Dalhousie University under the supervision of Jeff Dahn. His interests include multivalent and Li-ion batteries and, more generally, the electrochemistry and physical chemistry of liquid electrolytes for energy storage applications.



Bryan D. McCloskey is an Associate Professor and the Vice Chair of Graduate Education in the Department of Chemical and Biomolecular Engineering at the University of California, Berkeley, and also holds a joint appointment as a Faculty Engineer in the Energy Storage and Distributed Resources Division at Lawrence Berkeley National Laboratory. His laboratory currently focuses on a variety of challenges facing Li-ion and metal-air batteries, including high voltage cathode stability, advanced cathode material development, extreme fast charging, low temperature electrolyte formulations, and polyelectrolyte solution transport phenomena. More information about the McCloskey Lab can be found at the Lab's website: [www.mccloskeylab.com](http://www.mccloskeylab.com).



Kristin A. Persson obtained her Ph.D. in Theoretical Physics at the Royal Institute of Technology in Stockholm, Sweden, in 2001. She is a Professor in Materials Science and Engineering at UC Berkeley with a joint appointment as Senior Faculty Scientist at the Lawrence Berkeley National Laboratory. She is also a member of the UC Berkeley Kavli-ENSI Energy Nanoscience Institute. She is the Director and cofounder of the Materials Project ([www.materialsproject.org](http://www.materialsproject.org)), one of the most visible of the Materials Genome Initiative (MGI) funded programs attracting over a hundred thousand users worldwide. She is a leader in the MGI community and is known for her advancement of data-driven materials design and advancement of materials informatics. She is an Associate Editor for *Chemistry of Materials* and holds several patents in the clean energy space and has coauthored more than 200 peer-reviewed publications.

## ACKNOWLEDGMENTS

The authors thank Kranthi K. Mandadapu for guidance on the theoretical developments described in this work. K.D.F. acknowledges support from NSF GRFP under Grant DGE 1752814. J.S., B.D.M., and K.A.P. acknowledge support by the Assistant Secretary for Energy Efficiency and Renewable Energy, Vehicle Technologies Office, of the U.S. Department of Energy under Contract DE-AC02-05CH11231, under the Advanced Battery Materials Research (BMR) Program managed by Tien Duong.

## REFERENCES

- (1) Hallinan Jr, D. T.; Balsara, N. P. Polymer electrolytes. *Annu. Rev. Mater. Res.* **2013**, *43*, 503–525.
- (2) Agrawal, R.; Pandey, G. Solid polymer electrolytes: Materials designing and all-solid-state battery applications: an overview. *J. Phys. D: Appl. Phys.* **2008**, *41*, 223001.
- (3) Wang, Y.; Chen, K. S.; Mishler, J.; Cho, S. C.; Adroher, X. C. A review of polymer electrolyte membrane fuel cells: Technology, applications, and needs on fundamental research. *Appl. Energy* **2011**, *88*, 981–1007.
- (4) Neburchilov, V.; Martin, J.; Wang, H.; Zhang, J. A review of polymer electrolyte membranes for direct methanol fuel cells. *J. Power Sources* **2007**, *169*, 221–238.
- (5) Das, S.; Dutta, K.; Rana, D. Polymer electrolyte membranes for microbial fuel cells: a review. *Polym. Rev.* **2018**, *58*, 610–629.
- (6) Le, N. L.; Nunes, S. P. Materials and membrane technologies for water and energy sustainability. *Sustainable Materials and Technologies* **2016**, *7*, 1–28.
- (7) Yen, S. K.; Su, M.; Wang, K. Y.; Chung, T.-S.; et al. Study of draw solutes using 2-methylimidazole-based compounds in forward osmosis. *J. Membr. Sci.* **2010**, *364*, 242–252.
- (8) Bone, S. E.; Steinrück, H.-G.; Toney, M. F. Advanced characterization in clean water technologies. *Joule* **2020**, *4*, 1637–1659.
- (9) Werber, J. R.; Osuji, C. O.; Elimelech, M. Materials for next-generation desalination and water purification membranes. *Nat. Rev. Mater.* **2016**, *1*, 1–15.
- (10) Rubinstein, M.; Papoian, G. A. Polyelectrolytes in biology and soft matter. *Soft Matter* **2012**, *8*, 9265–9267.
- (11) Lankalapalli, S.; Kolapalli, V. Polyelectrolyte complexes: A review of their applicability in drug delivery technology. *Indian journal of pharmaceutical sciences* **2009**, *71*, 481.
- (12) Benner, S. A.; Hutter, D. Phosphates, DNA, and the search for nonterrestrial life: A second generation model for genetic molecules. *Bioorg. Chem.* **2002**, *30*, 62–80.
- (13) Arangundy-Franklin, S.; Taylor, A. I.; Porebski, B. T.; Genna, V.; Peak-Chew, S.; Vaisman, A.; Woodgate, R.; Orozco, M.; Holliger, P. Encoded synthesis and evolution of alkyl-phosphonate nucleic acids: A synthetic genetic polymer with an uncharged backbone chemistry. *Nat. Chem.* **2019**, *11*, 533.
- (14) Son, C. Y.; Wang, Z.-G. Ion transport in small-molecule and polymer electrolytes. *J. Chem. Phys.* **2020**, *153*, 100903.
- (15) Zhang, H.; Li, C.; Piszcz, M.; Coya, E.; Rojo, T.; Rodriguez-Martinez, L. M.; Armand, M.; Zhou, Z. Single lithium-ion conducting solid polymer electrolytes: advances and perspectives. *Chem. Soc. Rev.* **2017**, *46*, 797–815.
- (16) Diederichsen, K. M.; McShane, E. J.; McCloskey, B. D. Promising routes to a high Li<sup>+</sup> transference number electrolyte for lithium ion batteries. *ACS Energy Letters* **2017**, *2*, 2563–2575.
- (17) Newman, J.; Thomas-Alyea, K. E. *Electrochemical Systems*, 3rd ed.; John Wiley & Sons, Inc.: 2004.
- (18) Bird, R.; Stewart, W.; Lightfoot, E. *Transport Phenomena*; John Wiley & Sons, Inc.: 1960.
- (19) Krishna, R.; Wesselingh, J. The Maxwell-Stefan approach to mass transfer. *Chem. Eng. Sci.* **1997**, *52*, 861–911.
- (20) Villaluenga, I.; Pesko, D. M.; Timachova, K.; Feng, Z.; Newman, J.; Srinivasan, V.; Balsara, N. P. Negative Stefan-Maxwell diffusion coefficients and complete electrochemical transport characterization of homopolymer and block copolymer electrolytes. *J. Electrochem. Soc.* **2018**, *165*, A2766.
- (21) Choo, Y.; Halat, D. M.; Villaluenga, I.; Timachova, K.; Balsara, N. P. Diffusion and migration in polymer electrolytes. *Prog. Polym. Sci.* **2020**, *103*, 101220.
- (22) Wheeler, D. R.; Newman, J. Molecular dynamics simulations of multicomponent diffusion. I. Equilibrium method. *J. Phys. Chem. B* **2004**, *108*, 18353–18361.
- (23) Fong, K. D.; Bergstrom, H. K.; McCloskey, B. D.; Mandadapu, K. K. Transport phenomena in electrolyte solutions: Non-equilibrium thermodynamics and statistical mechanics. *AIChE J.* **2020**, *66*, e17091.
- (24) Onsager, L. Reciprocal relations in irreversible processes. I. *Phys. Rev.* **1931**, *37*, 405–426.
- (25) Onsager, L. Reciprocal relations in irreversible processes. II. *Phys. Rev.* **1931**, *38*, 2265–2279.
- (26) Prigogine, I. *Introduction to Thermodynamics of Irreversible Processes*, 3rd ed.; Interscience Publishers, Inc.: New York, 1967.
- (27) Hirschfelder, J. O.; Curtiss, C. F.; Bird, R. B.; Mayer, M. G. *Molecular Theory of Gases and Liquids*; John Wiley & Sons, Inc.: 1964; Vol. 165.
- (28) Katchalsky, A.; Curran, P. F. *Nonequilibrium Thermodynamics in Biophysics*; Harvard University Press: 1967.
- (29) Fong, K. D.; Self, J.; Diederichsen, K. M.; Wood, B. M.; McCloskey, B. D.; Persson, K. A. Ion transport and the true transference number in nonaqueous polyelectrolyte solutions for lithium ion batteries. *ACS Cent. Sci.* **2019**, *5*, 1250–1260.
- (30) Fong, K. D.; Self, J.; McCloskey, B. D.; Persson, K. A. Onsager transport coefficients and transference numbers in polyelectrolyte solutions and polymerized ionic liquids. *Macromolecules* **2020**, *53*, 9503–9512.
- (31) Wohde, F.; Balabajew, M.; Roling, B. Li<sup>+</sup> transference numbers in liquid electrolytes obtained by very-low-frequency impedance spectroscopy at variable electrode distances. *J. Electrochem. Soc.* **2016**, *163*, A714.

- (32) Vargas-Barbosa, N. M.; Roling, B. Dynamic ion correlations in solid and liquid electrolytes: How do they affect charge and mass transport? *ChemElectroChem* **2020**, *7*, 367–385.
- (33) Dong, D.; Bedrov, D. Charge transport in [Li (tetraglyme)][bis(trifluoromethane) sulfonimide] solvate ionic liquids: Insight from molecular dynamics simulations. *J. Phys. Chem. B* **2018**, *122*, 9994–10004.
- (34) McDaniel, J. G.; Son, C. Y. Ion correlation and collective dynamics in BMIM/BF<sub>4</sub>-based organic electrolytes: From dilute solutions to the ionic Liquid Limit. *J. Phys. Chem. B* **2018**, *122*, 7154–7169.
- (35) Bocharova, V.; Sokolov, A. P. Perspectives for polymer electrolytes: A view from fundamentals of ionic conductivity. *Macromolecules* **2020**, *53*, 4141–4157.
- (36) Gartner III, T. E.; Jayaraman, A. Modeling and simulations of polymers: A roadmap. *Macromolecules* **2019**, *52*, 755–786.
- (37) Mogurampelly, S.; Borodin, O.; Ganesan, V. Computer simulations of ion transport in polymer electrolyte membranes. *Annu. Rev. Chem. Biomol. Eng.* **2016**, *7*, 349–371.
- (38) Ganesan, V. Ion transport in polymeric ionic liquids: recent developments and open questions. *Molecular Systems Design & Engineering* **2019**, *4*, 280–293.
- (39) de Groot, S. R.; Mazur, P. *Non-Equilibrium Thermodynamics*; Interscience Publishers, Inc.: New York, 1969.
- (40) Boettcher, S. W.; Oener, S. Z.; Lonergan, M. C.; Surendranath, Y.; Ardo, S.; Brozek, C.; Kempler, P. A. Potentially confusing: Potentials in electrochemistry. *ACS Energy Letters* **2021**, *6*, 261–266.
- (41) Kjelstrup, S.; Bedeaux, D. *Non-equilibrium Thermodynamics of Heterogeneous Systems*; World Scientific: 2020; Vol. 20.
- (42) Zhang, Z.; Wheatle, B. K.; Krajniak, J.; Keith, J. R.; Ganesan, V. Ion mobilities, transference numbers, and inverse Haven ratios of polymeric ionic liquids. *ACS Macro Lett.* **2020**, *9*, 84–89.
- (43) Zhou, Y.; Miller, G. H. Green–Kubo formulas for mutual diffusion coefficients in multicomponent systems. *J. Phys. Chem.* **1996**, *100*, 5516–5524.
- (44) Sinnave, D. The Stejskal-Tanner equation generalized for any gradient shape—an overview of most pulse sequences measuring free diffusion. *Concepts Magn. Reson., Part A* **2012**, *40*, 39–65.
- (45) Grundy, L. S.; Shah, D. B.; Nguyen, H. Q.; Diederichsen, K. M.; Celik, H.; DeSimone, J. M.; McCloskey, B. D.; Balsara, N. P. Impact of frictional interactions on conductivity, diffusion, and transference number in ether-and perfluoroether-based electrolytes. *J. Electrochem. Soc.* **2020**, *167*, 120540.
- (46) Stejskal, E. O.; Tanner, J. E. Spin diffusion measurements: Spin echoes in the presence of a time-dependent field gradient. *J. Chem. Phys.* **1965**, *42*, 288–292.
- (47) Yoshida, K.; Tsuchiya, M.; Tachikawa, N.; Dokko, K.; Watanabe, M. Change from glyme solutions to quasi-ionic liquids for binary mixtures consisting of lithium bis(trifluoromethanesulfonyl) amide and glymes. *J. Phys. Chem. C* **2011**, *115*, 18384–18394.
- (48) Jamali, S. H.; Wolff, L.; Becker, T. M.; Bardow, A.; Vlucht, T. J.; Moulton, O. A. Finite-size effects of binary mutual diffusion coefficients from molecular dynamics. *J. Chem. Theory Comput.* **2018**, *14*, 2667–2677.
- (49) Trullas, J.; Padró, J. Diffusion in multicomponent liquids: A new set of collective velocity correlation functions and diffusion coefficients. *J. Chem. Phys.* **1993**, *99*, 3983–3989.
- (50) Shen, K.-H.; Hall, L. M. Ion conductivity and correlations in model salt-doped polymers: Effects of interaction strength and concentration. *Macromolecules* **2020**, *53*, 3655–3668.
- (51) Savoie, B. M.; Webb, M. A.; Miller III, T. F. Enhancing cation diffusion and suppressing anion diffusion via Lewis-acidic polymer electrolytes. *J. Phys. Chem. Lett.* **2017**, *8*, 641–646.
- (52) Hall, L. M.; Stevens, M. J.; Frischknecht, A. L. Dynamics of model ionomer melts of various architectures. *Macromolecules* **2012**, *45*, 8097–8108.
- (53) Zhang, H.; Chen, F.; Lakuntza, O.; Oteo, U.; Qiao, L.; Martinez-Ibañez, M.; Zhu, H.; Carrasco, J.; Forsyth, M.; Armand, M. Suppressed mobility of negative charges in polymer electrolytes with an ether-functionalized anion. *Angew. Chem.* **2019**, *131*, 12198–12203.
- (54) Webb, M. A.; Jung, Y.; Pesko, D. M.; Savoie, B. M.; Yamamoto, U.; Coates, G. W.; Balsara, N. P.; Wang, Z.-G.; Miller III, T. F. Systematic computational and experimental investigation of lithium-ion transport mechanisms in polyester-based polymer electrolytes. *ACS Cent. Sci.* **2015**, *1*, 198–205.
- (55) Barsoukov, E.; Macdonald, J. R. *Impedance Spectroscopy: Theory, Experiment, and Application*; John Wiley & Sons, Inc.: 2005.
- (56) Evans, J.; Vincent, C.; Bruce, P. Electrochemical measurement of transference numbers in polymer electrolytes. *Polymer* **1987**, *28*, 2324–2328.
- (57) Balsara, N. P.; Newman, J. Relationship between steady-state current in symmetric cells and transference number of electrolytes comprising univalent and multivalent ions. *J. Electrochem. Soc.* **2015**, *162*, A2720.
- (58) Bruce, P.; Hardgrave, M.; Vincent, C. The determination of transference numbers in solid polymer electrolytes using the Hittorf method. *Solid State Ionics* **1992**, *53–56*, 1087–1094.
- (59) Holz, M. Electrophoretic NMR. *Chem. Soc. Rev.* **1994**, *23*, 165–174.
- (60) Harned, H.; French, D. A conductance method for the determination of the diffusion coefficients of electrolytes. *Ann. N. Y. Acad. Sci.* **1945**, *46*, 267–284.
- (61) Ma, Y.; Doyle, M.; Fuller, T. F.; Doeff, M. M.; De Jonghe, L. C.; Newman, J. The measurement of a complete set of transport properties for a concentrated solid polymer electrolyte solution. *J. Electrochem. Soc.* **1995**, *142*, 1859.
- (62) Hansen, J.-P.; McDonald, I. R. *Theory of Simple Liquids*; Elsevier: 1990.
- (63) Frenkel, D.; Smit, B. *Understanding Molecular Simulation: From Algorithms to Applications*, 2nd ed.; Academic Press: 2001; Vol. 50.
- (64) Harris, K. R. On the use of the Angell-Walden equation to determine the “ionicity” of molten salts and ionic liquids. *J. Phys. Chem. B* **2019**, *123*, 7014–7023.
- (65) MacFarlane, D. R.; Forsyth, M.; Izgorodina, E. I.; Abbott, A. P.; Annat, G.; Fraser, K. On the concept of ionicity in ionic liquids. *Phys. Chem. Chem. Phys.* **2009**, *11*, 4962–4967.
- (66) Nilsson, V.; Bernin, D.; Brandell, D.; Edström, K.; Johansson, P. Interactions and transport in highly concentrated LiTFSI-based electrolytes. *ChemPhysChem* **2020**, *21*, 1166–1176.
- (67) Murch, G. The Haven ratio in fast ionic conductors. *Solid State Ionics* **1982**, *7*, 177–198.
- (68) Kisliuk, A.; Bocharova, V.; Popov, I.; Gainaru, C.; Sokolov, A. P. Fundamental parameters governing ion conductivity in polymer electrolytes. *Electrochim. Acta* **2019**, *299*, 191–196.
- (69) Li, Z.; Smith, G. D.; Bedrov, D. Li<sup>+</sup> solvation and transport properties in ionic liquid/lithium salt mixtures: A molecular dynamics simulation study. *J. Phys. Chem. B* **2012**, *116*, 12801–12809.
- (70) Borodin, O.; Gorecki, W.; Smith, G. D.; Armand, M. Molecular dynamics simulation and pulsed-field gradient NMR studies of bis(fluorosulfonyl)imide (FSI) and bis[(trifluoromethyl)sulfonyl]-imide (TFSI)-based ionic liquids. *J. Phys. Chem. B* **2010**, *114*, 6786–6798.
- (71) Lesch, V.; Jeremias, S.; Moretti, A.; Passerini, S.; Heuer, A.; Borodin, O. A combined theoretical and experimental study of the influence of different anion ratios on lithium ion dynamics in ionic liquids. *J. Phys. Chem. B* **2014**, *118*, 7367–7375.
- (72) Doyle, M.; Fuller, T. F.; Newman, J. Modeling of galvanostatic charge and discharge of the lithium/polymer/insertion cell. *J. Electrochem. Soc.* **1993**, *140*, 1526.
- (73) Crothers, A. R.; Darling, R. M.; Kusoglu, A.; Radke, C. J.; Weber, A. Z. Theory of multicomponent phenomena in cation-exchange membranes: Part II. Transport model and validation. *J. Electrochem. Soc.* **2020**, *167*, 013548.
- (74) Schammer, M.; Horstmann, B.; Latz, A. Theory of transport in highly concentrated electrolytes. *arXiv preprint arXiv:2010.14915*, 2020.

- (75) Smith, R. B.; Bazant, M. Z. Multiphase porous electrode theory. *J. Electrochem. Soc.* **2017**, *164*, E3291.
- (76) Liu, X.; Vlugt, T. J.; Bardow, A. Predictive Darken equation for Maxwell-Stefan diffusivities in multicomponent mixtures. *Ind. Eng. Chem. Res.* **2011**, *50*, 10350–10358.
- (77) Krishna, R.; Van Baten, J. The Darken relation for multi-component diffusion in liquid mixtures of linear alkanes: an investigation using molecular dynamics (MD) simulations. *Ind. Eng. Chem. Res.* **2005**, *44*, 6939–6947.
- (78) Van De Ven-Lucassen, I. M.; Thijs, J. V. A. J. V.; Der Zanden, P. J. K. Using molecular dynamics to obtain Maxwell-Stefan diffusion coefficients in liquid systems. *Mol. Phys.* **1998**, *94*, 495–503.
- (79) van de Ven-Lucassen, I. M.; Otten, A. M.; Vlugt, T. J.; Kerkhof, P. J. Molecular dynamics simulation of the Maxwell-Stefan diffusion coefficients in Lennard-Jones liquid mixtures. *Mol. Simul.* **1999**, *23*, 43–54.
- (80) Marcus, Y.; Hefter, G. Ion pairing. *Chem. Rev.* **2006**, *106*, 4585–4621.
- (81) Ravikumar, B.; Mynam, M.; Rai, B. Effect of salt concentration on properties of lithium ion battery electrolytes: A molecular dynamics study. *J. Phys. Chem. C* **2018**, *122*, 8173–8181.
- (82) Samuel, D.; Steinhauser, C.; Smith, J. G.; Kaufman, A.; Radin, M. D.; Naruse, J.; Hiramatsu, H.; Siegel, D. J. Ion pairing and diffusion in magnesium electrolytes based on magnesium borohydride. *ACS Appl. Mater. Interfaces* **2017**, *9*, 43755–43766.
- (83) France-Lanord, A.; Grossman, J. C. Correlations from ion pairing and the Nernst-Einstein equation. *Phys. Rev. Lett.* **2019**, *122*, 136001.
- (84) Burlatsky, S.; Darling, R. M.; Novikov, D.; Atrazhev, V. V.; Sultanov, V. I.; Astakhova, T. Y.; Su, L.; Brushett, F. Molecular dynamics modeling of the conductivity of lithiated Nafion containing nonaqueous solvents. *J. Electrochem. Soc.* **2016**, *163*, A2232.
- (85) Manning, G. S. Limiting laws and counterion condensation in polyelectrolyte solutions II. Self-diffusion of the small ions. *J. Chem. Phys.* **1969**, *51*, 934–938.
- (86) Vink, H. *Physical Chemistry of Polyelectrolytes*, 1st ed.; CRC Press: Boca Raton, FL, 2001; Chapter 7, pp 225–244.
- (87) Colby, R. H.; Boris, D. C.; Krause, W. E.; Tan, J. S. Polyelectrolyte conductivity. *J. Polym. Sci., Part B: Polym. Phys.* **1997**, *35*, 2951–2960.
- (88) Muthukumar, M. Ordinary-extraordinary transition in dynamics of solutions of charged macromolecules. *Proc. Natl. Acad. Sci. U. S. A.* **2016**, *113*, 12627–12632.
- (89) Muthukumar, M. 50th anniversary perspective: A perspective on polyelectrolyte solutions. *Macromolecules* **2017**, *50*, 9528–9560.
- (90) Dobrynin, A. V.; Colby, R. H.; Rubinstein, M. Scaling theory of polyelectrolyte solutions. *Macromolecules* **1995**, *28*, 1859–1871.
- (91) Payne, V. A.; Lonergan, M. C.; Forsyth, M.; Ratner, M. A.; Shriver, D. F.; de Leeuw, S. W.; Perram, J. W. Simulations of structure and transport in polymer electrolytes. *Solid State Ionics* **1995**, *81*, 171–181.
- (92) Harris, K. R. Relations between the fractional Stokes-Einstein and Nernst-Einstein equations and velocity correlation coefficients in ionic liquids and molten salts. *J. Phys. Chem. B* **2010**, *114*, 9572–9577.
- (93) Kamcev, J.; Paul, D. R.; Manning, G. S.; Freeman, B. D. Ion diffusion coefficients in ion exchange membranes: significance of counterion condensation. *Macromolecules* **2018**, *51*, 5519–5529.
- (94) Mogurampelly, S.; Keith, J. R.; Ganesan, V. Mechanisms underlying ion transport in polymerized ionic liquids. *J. Am. Chem. Soc.* **2017**, *139*, 9511–9514.
- (95) Frischknecht, A. L.; Paren, B. A.; Middleton, L. R.; Koski, J. P.; Tarver, J. D.; Tyagi, M.; Soles, C. L.; Winey, K. I. Chain and ion dynamics in precise polyethylene ionomers. *Macromolecules* **2019**, *52*, 7939–7950.
- (96) Ma, B.; Nguyen, T. D.; Olvera de la Cruz, M. Control of ionic mobility via charge size asymmetry in random ionomers. *Nano Lett.* **2020**, *20*, 43–49.
- (97) Bollinger, J. A.; Stevens, M. J.; Frischknecht, A. L. Quantifying single-ion transport in percolated ionic aggregates of polymer melts. *ACS Macro Lett.* **2020**, *9*, 583–587.
- (98) Buss, H. G.; Chan, S. Y.; Lynd, N. A.; McCloskey, B. D. Nonaqueous polyelectrolyte solutions as liquid electrolytes with high lithium ion transference number and conductivity. *ACS Energy Letters* **2017**, *2*, 481–487.
- (99) Aihara, Y.; Sugimoto, K.; Price, W. S.; Hayamizu, K. Ionic conduction and self-diffusion near infinitesimal concentration in lithium salt-organic solvent electrolytes. *J. Chem. Phys.* **2000**, *113*, 1981–1991.
- (100) Borodin, O.; Smith, G. D. Mechanism of ion transport in amorphous poly(ethylene oxide)/LiTFSI from molecular dynamics simulations. *Macromolecules* **2006**, *39*, 1620–1629.
- (101) Picalek, J.; Kolafa, J. Molecular dynamics study of conductivity of ionic liquids: The Kohlrausch law. *J. Mol. Liq.* **2007**, *134*, 29–33.
- (102) Hayamizu, K. Temperature dependence of self-diffusion coefficients of ions and solvents in ethylene carbonate, propylene carbonate, and diethyl carbonate single solutions and ethylene carbonate + diethyl carbonate binary solutions of LiPF<sub>6</sub> studied by NMR. *J. Chem. Eng. Data* **2012**, *57*, 2012–2017.
- (103) Diederichsen, K. M.; Fong, K. D.; Terrell, R. C.; Persson, K. A.; McCloskey, B. D. Investigation of solvent type and salt addition in high transference number nonaqueous polyelectrolyte solutions for lithium ion batteries. *Macromolecules* **2018**, *51*, 8761–8771.
- (104) Gebbie, M. A.; Valtiner, M.; Banquy, X.; Fox, E. T.; Henderson, W. A.; Israelachvili, J. N. Ionic liquids behave as dilute electrolyte solutions. *Proc. Natl. Acad. Sci. U. S. A.* **2013**, *110*, 9674–9679.
- (105) Lee, A. A.; Perez-Martinez, C. S.; Smith, A. M.; Perkin, S. Scaling analysis of the screening length in concentrated electrolytes. *Phys. Rev. Lett.* **2017**, *119*, 026002.
- (106) Jones, P.; Coupette, F.; Härtel, A.; Lee, A. A. Bayesian unsupervised learning reveals hidden structure in concentrated electrolytes. *arXiv preprint arXiv:2012.10694*, 2020.
- (107) Self, J.; Fong, K. D.; Persson, K. A. Transport in super-concentrated LiPF<sub>6</sub> and LiBF<sub>4</sub>/propylene carbonate electrolytes. *ACS Energy Letters* **2019**, *4*, 2843–2849.
- (108) Solano, C. J.; Jeremias, S.; Paillard, E.; Beljonne, D.; Lazzaroni, R. A joint theoretical/experimental study of the structure, dynamics, and Li<sup>+</sup> transport in bis([tri]fluoro[methane]sulfonyl)imide [T]FSI-based ionic liquids. *J. Chem. Phys.* **2013**, *139*, 034502.
- (109) Borodin, O.; Smith, G. D.; Henderson, W. Li<sup>+</sup> cation environment, transport, and mechanical properties of the LiTFSI doped N-methyl-N-alkylpyrrolidinium<sup>+</sup>TFSI<sup>-</sup> ionic liquids. *J. Phys. Chem. B* **2006**, *110*, 16879–16886.
- (110) Rosenwinkel, M. P.; Schönhoff, M. Lithium transference numbers in PEO/LiTFSI electrolytes determined by electrophoretic NMR. *J. Electrochem. Soc.* **2019**, *166*, A1977.
- (111) Schmidt, F.; Schönhoff, M. Solvate cation migration and ion correlations in solvate ionic liquids. *J. Phys. Chem. B* **2020**, *124*, 1245–1252.
- (112) Cheng, Y.; Yang, J.; Hung, J.-H.; Patra, T. K.; Simmons, D. S. Design rules for highly conductive polymeric ionic liquids from molecular dynamics simulations. *Macromolecules* **2018**, *51*, 6630–6644.
- (113) Yeager, H.; Kratochvil, B. Conductance study of ion pairing of alkali metal tetrafluoroborates and hexafluorophosphates in acetonitrile. *Can. J. Chem.* **1975**, *53*, 3448–3451.
- (114) Molinari, N.; Mailoa, J. P.; Kozinsky, B. Effect of salt concentration on ion clustering and transport in polymer solid electrolytes: A molecular dynamics study of PEO-LiTFSI. *Chem. Mater.* **2018**, *30*, 6298–6306.
- (115) Lin, K.-J.; Maranas, J. K. Does decreasing ion-ion association improve cation mobility in single ion conductors? *Phys. Chem. Chem. Phys.* **2013**, *15*, 16143–16151.
- (116) Shen, K.-H.; Hall, L. M. Effects of ion size and dielectric constant on ion transport and transference number in polymer electrolytes. *Macromolecules* **2020**, *53*, 10086–10096.
- (117) Ue, M. Mobility and ionic association of lithium and quaternary ammonium salts in propylene carbonate and  $\gamma$ -butyrolactone. *J. Electrochem. Soc.* **1994**, *141*, 3336.



- (118) Tominaga, Y.; Yamazaki, K.; Nanthana, V. Effect of anions on lithium ion conduction in poly (ethylene carbonate)-based polymer electrolytes. *J. Electrochem. Soc.* **2015**, *162*, A3133.
- (119) Zhang, Z.; Cui, Z.; Qiao, L.; Guan, J.; Xu, H.; Wang, X.; Hu, P.; Du, H.; Li, S.; Zhou, X.; et al. Novel design concepts of efficient Mg-ion electrolytes toward high-performance magnesium-selenium and magnesium-sulfur batteries. *Adv. Energy Mater.* **2017**, *7*, 1602055.
- (120) Shyamsunder, A.; Blanc, L. E.; Assoud, A.; Nazar, L. F. Reversible calcium plating and stripping at room temperature using a borate salt. *ACS Energy Letters* **2019**, *4*, 2271–2276.
- (121) Hahn, N. T.; Driscoll, D. M.; Yu, Z.; Sterbinsky, G. E.; Cheng, L.; Balasubramanian, M.; Zavadil, K. R. The influence of ether solvent and anion coordination on electrochemical behavior in calcium battery electrolytes. *ACS Applied Energy Materials* **2020**, *3*, 8437–8447.
- (122) Li, Z.; Fuhr, O.; Fichtner, M.; Zhao-Karger, Z. Towards stable and efficient electrolytes for room-temperature rechargeable calcium batteries. *Energy Environ. Sci.* **2019**, *12*, 3496–3501.
- (123) Ma, Q.; Xia, Y.; Feng, W.; Nie, J.; Hu, Y.-S.; Li, H.; Huang, X.; Chen, L.; Armand, M.; Zhou, Z. Impact of the functional group in the polyanion of single lithium-ion conducting polymer electrolytes on the stability of lithium metal electrodes. *RSC Adv.* **2016**, *6*, 32454–32461.
- (124) Mezziane, R.; Bonnet, J.-P.; Courty, M.; Djellab, K.; Armand, M.; et al. Single lithium-ion conducting polymer electrolytes based on a super-delocalized polyanion. *Angew. Chem., Int. Ed.* **2016**, *55*, 2521–2525.
- (125) Mezziane, R.; Bonnet, J.-P.; Courty, M.; Djellab, K.; Armand, M. Single-ion polymer electrolytes based on a delocalized polyanion for lithium batteries. *Electrochim. Acta* **2011**, *57*, 14–19.
- (126) Ito, K.; Ohno, H. Design of highly ion conductive polyether/salt hybrids. *Electrochim. Acta* **1998**, *43*, 1247–1252.
- (127) Benrabah, D.; Sylla, S.; Alloin, F.; Sanchez, J.-Y.; Armand, M. Perfluorosulfonate-polyether based single ion conductors. *Electrochim. Acta* **1995**, *40*, 2259–2264.
- (128) Kim, H.-T.; Park, J.-K. Effects of cations on ionic states of poly (oligo-oxethylene methacrylate-co-alkali metal acrylamidocaproate) single-ion conductor. *Solid State Ionics* **1997**, *98*, 237–244.
- (129) Kashyap, H. K.; Annapureddy, H. V.; Raineri, F. O.; Margulis, C. J. How is charge transport different in ionic liquids and electrolyte solutions? *J. Phys. Chem. B* **2011**, *115*, 13212–13221.
- (130) Feng, S.; Shi, D.; Liu, F.; Zheng, L.; Nie, J.; Feng, W.; Huang, X.; Armand, M.; Zhou, Z. Single lithium-ion conducting polymer electrolytes based on poly [(4-styrenesulfonyl)-(trifluoromethanesulfonyl) imide] anions. *Electrochim. Acta* **2013**, *93*, 254–263.
- (131) Bouchet, R.; Maria, S.; Mezziane, R.; Aboulaich, A.; Lienafa, L.; Bonnet, J.-P.; Phan, T. N.; Bertin, D.; Gimes, D.; Devaux, D.; et al. Single-ion BAB triblock copolymers as highly efficient electrolytes for lithium-metal batteries. *Nat. Mater.* **2013**, *12*, 452–457.
- (132) Porcarelli, L.; Shaplov, A. S.; Salsamendi, M.; Nair, J. R.; Vygodskii, Y. S.; Mecerreyes, D.; Gerbaldi, C. Single-ion block copoly (ionic liquid) s as electrolytes for all-solid state lithium batteries. *ACS Appl. Mater. Interfaces* **2016**, *8*, 10350–10359.
- (133) Li, S.; Mohamed, A. I.; Pande, V.; Wang, H.; Cuthbert, J.; Pan, X.; He, H.; Wang, Z.; Viswanathan, V.; Whitacre, J. F.; et al. Single-ion homopolymer electrolytes with high transference number prepared by click chemistry and photoinduced metal-free atom-transfer radical polymerization. *ACS Energy Letters* **2018**, *3*, 20–27.
- (134) Doyle, M.; Fuller, T. F.; Newman, J. The importance of the lithium ion transference number in lithium/polymer cells. *Electrochim. Acta* **1994**, *39*, 2073–2081.
- (135) Drifford, M.; Dalbiez, J. Dynamics of polyelectrolyte solutions by light scattering. *J. Phys., Lett.* **1985**, *46*, 311–319.
- (136) Förster, S.; Schmidt, M. *Physical Properties of Polymers*; Springer: 1995; pp 51–133.
- (137) Dewing, B. L.; Bible, N. G.; Ellison, C. J.; Mahanthappa, M. K. Electrochemically stable, high transference number lithium bis (malonate) borate polymer solution electrolytes. *Chem. Mater.* **2020**, *32*, 3794–3804.
- (138) Zhang, W.; Feng, S.; Huang, M.; Qiao, B.; Shigenobu, K.; Giordano, L.; Lopez, J.; Tataru, R.; Ueno, K.; Dokko, K. Molecularly tunable polyanions for single-ion conductors and poly (solvate ionic liquids). *Chem. Mater.* **2021**, *33*, 524.
- (139) Abbott, L. J.; Lawson, J. W. Effects of side chain length on ionic aggregation and dynamics in polymer single-ion conductors. *Macromolecules* **2019**, *52*, 7456–7467.
- (140) Ting, C. L.; Stevens, M. J.; Frischknecht, A. L. Structure and dynamics of coarse-grained ionomer melts in an external electric field. *Macromolecules* **2015**, *48*, 809–818.
- (141) Chen, X.; Chen, F.; Liu, M. S.; Forsyth, M. Polymer architecture effect on sodium ion transport in PSTFSI-based ionomers: A molecular dynamics study. *Solid State Ionics* **2016**, *288*, 271–276.
- (142) Timachova, K.; Chintapalli, M.; Olson, K. R.; Mecham, S. J.; DeSimone, J. M.; Balsara, N. P. Mechanism of ion transport in perfluoropolyether electrolytes with a lithium salt. *Soft Matter* **2017**, *13*, 5389–5396.
- (143) Timachova, K.; Watanabe, H.; Balsara, N. P. Effect of molecular weight and salt concentration on ion transport and the transference number in polymer electrolytes. *Macromolecules* **2015**, *48*, 7882–7888.
- (144) Lascaud, S.; Perrier, M.; Vallee, A.; Besner, S.; Prud'Homme, J.; Armand, M. Phase diagrams and conductivity behavior of poly (ethylene oxide)-molten salt rubbery electrolytes. *Macromolecules* **1994**, *27*, 7469–7477.
- (145) Wheatle, B. K.; Lynd, N. A.; Ganesan, V. Effect of polymer polarity on ion transport: a competition between ion aggregation and polymer segmental dynamics. *ACS Macro Lett.* **2018**, *7*, 1149–1154.
- (146) Wheatle, B. K.; Fuentes, E. F.; Lynd, N. A.; Ganesan, V. Influence of host polarity on correlating salt concentration, molecular weight, and molar conductivity in polymer electrolytes. *ACS Macro Lett.* **2019**, *8*, 888–892.
- (147) Pesko, D. M.; Timachova, K.; Bhattacharya, R.; Smith, M. C.; Villaluenga, I.; Newman, J.; Balsara, N. P. Negative transference numbers in poly (ethylene oxide)-based electrolytes. *J. Electrochem. Soc.* **2017**, *164*, E3569.
- (148) Gouverneur, M.; Schmidt, F.; Schönhoff, M. Negative effective Li transference numbers in Li salt/ionic liquid mixtures: Does Li drift in the “wrong” direction? *Phys. Chem. Chem. Phys.* **2018**, *20*, 7470–7478.
- (149) France-Lanord, A.; Wang, Y.; Xie, T.; Johnson, J. A.; Shao-Horn, Y.; Grossman, J. C. Effect of chemical variations in the structure of poly (ethylene oxide)-based polymers on lithium transport in concentrated electrolytes. *Chem. Mater.* **2020**, *32*, 121–126.
- (150) Joshi, Y.; Kwak, J. C. Transference numbers, polyion mobilities, and charge fractions in aqueous solutions of lithium, sodium, and potassium dextran sulfate. *Biophys. Chem.* **1980**, *12*, 323–328.
- (151) Jordan, D.; Kurucsev, T.; Martin, M. Comparative physical chemical study of isotactic and atactic poly (styrene sulphonic acid) solutions. Part 2. Electrical conductance and transference measurements in salt-free aqueous solutions. *Trans. Faraday Soc.* **1969**, *65*, 606–611.
- (152) De, R.; Lee, H.; Das, B. Exploring the interactions in binary mixtures of polyelectrolytes: Influence of mixture composition, concentration, and temperature on counterion condensation. *J. Mol. Liq.* **2018**, *251*, 94–99.
- (153) Kuznetsov, I.; Vorontsova, O.; Kozlov, A. Polyelectrolyte properties of biopolymers: Conductivity and secondary structure of polyriboadenylic acid and its salts in solutions. *Biopolymers* **1991**, *31*, 65–76.
- (154) Overbeek, J. T. G. *Macromolecular Chemistry-11*; Elsevier: 1977; pp 91–101.
- (155) Wheatle, B. K.; Keith, J. R.; Mogurampelly, S.; Lynd, N. A.; Ganesan, V. Influence of dielectric constant on ionic transport in polyether-based electrolytes. *ACS Macro Lett.* **2017**, *6*, 1362–1367.
- (156) Borodin, O.; Douglas, R.; Smith, G.; Eyring, E. M.; Petrucci, S. Microwave dielectric relaxation, electrical conductance, and ultrasonic relaxation of LiPF<sub>6</sub> in poly (ethylene oxide) dimethyl ether-500. *J. Phys. Chem. B* **2002**, *106*, 2140–2145.

(157) Petrucci, S.; Masiker, M. C.; Eyring, E. M. The possible presence of triple ions in electrolyte solutions of low dielectric permittivity. *J. Solution Chem.* **2008**, *37*, 1031–1035.

(158) Choi, U. H.; Liang, S.; Chen, Q.; Runt, J.; Colby, R. H. Segmental dynamics and dielectric constant of polysiloxane polar copolymers as plasticizers for polymer electrolytes. *ACS Appl. Mater. Interfaces* **2016**, *8*, 3215–3225.

(159) Gudla, H.; Zhang, C.; Brandell, D. Effects of solvent polarity on Li-ion diffusion in polymer electrolytes: An all-atom molecular dynamics study with charge scaling. *J. Phys. Chem. B* **2020**, *124*, 8124–8131.

(160) McBreen, J.; Lee, H.; Yang, X.; Sun, X. New approaches to the design of polymer and liquid electrolytes for lithium batteries. *J. Power Sources* **2000**, *89*, 163–167.

(161) Bard, A. J.; Faulkner, L. R.; et al. Fundamentals and applications. *Electrochemical Methods* **2001**, *2*, 580–632.